Monthly Notices
of the
ROYAL ASTRONOMICAL SOCIETY

Mon. Not. R. Astron. Soc. **408,** 1606–1622 (2010) doi:10.1111/j.1365-2966.2010.17233.x

Estimating the masses of extra-solar planets

C. A. Watson,[1⋆] S. P. Littlefair,[2] A. Collier Cameron,[3] V. S. Dhillon[2] and E. K. Simpson[1]

[1]*Astrophysics Research Centre, School of Mathematics & Physics, Queen's University, University Road, Belfast BT7 1NN*
[2]*Department of Physics and Astronomy, University of Sheffield, Sheffield S3 7RH*
[3]*School of Physics and Astronomy, University of St Andrews, North Haugh, St Andrews, Fife KY19 9SS*

Accepted 2010 June 19. Received 2010 June 18; in original form 2009 September 17

ABSTRACT

All extra-solar planet masses that have been derived spectroscopically are lower limits since the inclination of the orbit to our line-of-sight is unknown except for transiting systems. In theory, however, it is possible to determine the inclination angle, i, between the rotation axis of a star and an observer's line-of-sight from measurements of the projected equatorial velocity ($v \sin i$), the stellar rotation period ($P_{\rm rot}$) and the stellar radius (R_*). For stars which host planetary systems this allows the removal of the $\sin i$ dependency of extra-solar planet masses derived from spectroscopic observations under the assumption that the planetary orbits lie perpendicular to the stellar rotation axis.

We have carried out an extensive literature search and present a catalogue of $v \sin i$, $P_{\rm rot}$ and R_* estimates for stars hosting extra-solar planets. In addition, we have used *Hipparcos* parallaxes and the Barnes–Evans relationship to further supplement the R_* estimates obtained from the literature. Using this catalogue, we have obtained $\sin i$ estimates using a Markov-chain Monte Carlo analysis. This technique allows proper 1σ two-tailed confidence limits to be placed on the derived $\sin i$'s along with the transit probability for each planet to be determined.

While we find that a small proportion of systems yield $\sin i$'s significantly greater than 1, most likely due to poor $P_{\rm rot}$ estimations, the large majority are acceptable. We are further encouraged by the cases where we have data on transiting systems, as the technique indicates inclinations of $\sim 90^\circ$ and high transit probabilities. In total, we are able to estimate the true masses of 133 extra-solar planets. Of these 133 extra-solar planets, only six have revised masses that place them above the $13 M_{\rm J}$ deuterium burning limit; four of those six extra-solar planet candidates were already suspected to lie above the deuterium burning limit before correcting their masses for the $\sin i$ dependency. Our work reveals a population of high-mass extra-solar planets with low eccentricities, and we speculate that these extra-solar planets may represent the signature of different planetary formation mechanisms at work. Finally, we discuss future observations that should improve the robustness of this technique.

Key words: stars: fundamental parameters – planetary systems – stars: rotation.

1 INTRODUCTION

Over 16 years ago, the first planets to be detected outside of our Solar system were discovered around the millisecond pulsar PSR 1257+12 (Wolszcan & Frail 1992). Within 3 years, Mayor & Queloz (1995) announced the first planet orbiting around a main-sequence star, 51 Peg b. Since then, extra-solar planet candidates have been discovered at a phenomenal rate. At the time of writing, 453 extra-solar planet candidates have now been identified through a variety of techniques including radial velocity studies, transits, microlensing events, stellar pulsations and pulsar timing.

By far, the most extra-solar planets have been discovered by observing the small Doppler wobble of the host star. This technique, however, only returns a minimum mass $M \sin i$ (where M is the mass of the planet and i is the inclination of the normal to the planetary orbital plane to the observer's line-of-sight), which is a firm lower limit to the true planetary mass. Indeed, the inclination (and hence true planetary mass) can only be determined accurately for those planets which transit their host star. With only $\sim$70 transiting planets

⋆E-mail: c.a.watson@qub.ac.uk

known, this leaves the vast majority of planets with only lower limits placed on their masses. Improving the mass determinations of these planets has obvious benefits for planet formation modelling and for studying the planet mass distribution.

In this paper, we present a method for estimating the orbital inclinations and hence true masses of non-transiting extra-solar planets. We then apply this method to the extra-solar planet systems for which there is sufficient data available, and investigate the impact that the corrected masses have on our knowledge of extra-solar planet properties. Finally, we conclude with a look at the improved measurements that should be taken to make this technique more robust.

2 ESTIMATING THE ORBITAL INCLINATIONS OF EXTRA-SOLAR PLANETS

It is possible to determine the inclination angle, i, between the rotation axis of the extra-solar planet host star and the observer's line-of-sight. By combining measurements of the star's projected equatorial velocity ($v \sin i$), the stellar rotation period ($P_{\rm rot}$) and the stellar radius (R_*), one can determine $\sin i$ from

$$\sin i = \frac{P_{\rm rot} \times v \sin i}{2\pi R_*}. \quad (1)$$

Indeed, this method has previously been applied by Gonzalez (1998) to seven exoplanet host stars, as well as by Cameron & Foing (1997) to determine the inclination of the rotation axis of the extensively Doppler-imaged young star AB Dor, for example. Equation (1) can then be used to lift the $\sin i$ degeneracy in calculating extra-solar planet masses using spectroscopic observations if it is assumed that the planetary orbits lie perpendicular to the host star's rotation axis. Certainly, this condition holds true for our Solar system, which has an angle between the plane of the ecliptic and the solar equator of around 7° (Beck & Giles 2005). The degree of alignment between the stellar spin axis and the planetary orbit can also be measured for transiting extra-solar planets using the Rossiter–McLaughlin effect (e.g. Gaudi & Winn 2007). So far, this has been carried out for 26 planet systems (see Winn et al. 2005, 2007; Wolf et al. 2007; Narita et al. 2007; Johnson et al. 2008; Cochran et al. 2008; Hébrard et al. 2008; Bouchy et al. 2008; Winn et al. 2008; Johnson et al. 2009; Winn et al. 2009b; Narita et al. 2009b; Pont et al. 2009; Triaud et al. 2009; Gillon et al. 2009; Narita et al. 2010; Anderson et al. 2010; Jenkins et al. 2010; Simpson et al. 2010; Queloz et al. 2010; Triaud et al. 2010).

Of these 26 systems, seven appear to have appreciable misalignment angles. These are HD 80606b, XO-3b, HAT-P-7b, WASP-2b, WASP-8b, WASP-14b, WASP-15b and WASP-17b. While Hébrard et al. (2008) initially suggested that the spin–orbit misalignment measured for XO-3 may be due to a systematic error as a result of the high airmass at which their observations were carried out, Winn et al. (2009a) have since confirmed the misalignment. We should also note that at first the spin–orbit misalignment of HD 17156 was measured to be $62° \pm 25°$ by Narita et al. (2008), but that subsequent work by Cochran et al. (2008) and Narita et al. (2009a) has since concluded that the planetary orbital axis is, in fact, well aligned with the stellar rotation axis. Pont et al. (2009) have reported a $\sim 50°$ misalignment in HD 80606. This system is a binary, and the misalignment may well arise through the action of the Kozai mechanism (e.g. Takeda & Rasio 2005; Malmberg, Davies & Chambers 2007). HD 80606b also exhibits a large orbital eccentricity, no doubt as a result of the Kozai interactions. In addition, WASP-8b is part of a triple system (Queloz et al. 2010) and therefore its mis-alignment angle is also most likely due to the Kozai mechanism. This leaves four planetary systems with confirmed mis-alignment angles for which no stellar companion is yet known. Whether the Kozai mechanism is a dominant process affecting the orbital evolution of exoplanets in non-binary systems is yet to be seen, but obviously some caution must be applied when assuming spin–orbit alignment. For now, however, we will work on the premise that this assumption is a reasonable one for single stars.

In order to measure the orbital inclination of extra-solar planets, we can see from equation (1) that we require just three quantities, $v \sin i$, R_* and $P_{\rm rot}$. The projected stellar equatorial rotation-velocity, $v \sin i$, can be measured using high-resolution spectroscopy. While the stars targeted by extra-solar planet hunts are generally slowly rotating (in order to avoid spurious radial velocities introduced by magnetic activity generated in rapidly rotating stars), the spectrographs used for hunting extra-solar planets are high-resolution instruments. Thus, most extra-solar planet host stars have their line-broadening measured. One possible caveat with these measurements is that the stellar rotation may no longer be considered the sole line-broadening mechanism and other mechanisms, such as turbulence (see Section 8 for a discussion), may have to be taken into account.

The radii of the extra-solar planet host stars can be estimated in a variety of ways. While some stars may have their radii measured directly via interferometry, lunar occultations or transits/eclipses (e.g. Fracassini et al. 2001), the majority are estimated using indirect methods. The most common method is to combine stellar luminosities derived from bolometric corrections and *Hipparcos* parallaxes with effective temperatures (determined from spectral synthesis modelling) to determine the stellar radii. Indeed, Fischer & Valenti (2005) have done exactly this for a large number of extra-solar planet host stars, and quote a median error on the radii of ~3 per cent.

In addition to the published values of the stellar radii, we have also used the Barnes–Evans technique to estimate the angular diameters of the extra-solar planet host stars. We have used the $(V - K)$ colour–angular diameter relation of Fouque & Gieren (1997), who established the following empirical surface brightness ($F_{\rm v}$)–colour relationship:

$$F_{\rm v} = 3.947 - 0.131\,(V - K)\,. \quad (2)$$

When combined with the absolute visual magnitude, $M_{\rm v}$, the surface brightness parameter $F_{\rm v}$ calculated in equation (2) can be used to determine the radius of the star, in solar radii, using equation (2) of Beuermann, Baraffe & Hauschildt (1999):

$$R_* = 10^{0.2\times[42.368-(10\times F_{\rm v})-M_{\rm v}]}. \quad (3)$$

Thus, only the $M_{\rm v}$ of the host star is required, which can be calculated from the V-band magnitude and parallax measurements from *Hipparcos*. We have also taken into account extinction using the reddening law from Fouque & Gieren (1997):

$$E(V - K) = 0.88 A_{\rm v}, \quad (4)$$

and the absorption law from di Benedetto & Rabbia (1987):

$$A_{\rm v} = 0.14 \times \frac{1 - \exp(-10 \times d \times |\sin b|)}{|\sin b|}, \quad (5)$$

where $A_{\rm v}$ is the visual absorption coefficient, $E(V - K)$ the $V - K$ colour extinction, d the distance to the star in kpc and b the Galactic latitude. We note that the stellar radii and associated error bars we derive from the Barnes–Evans technique are in excellent agreement with the published stellar radii for extra-solar planet host stars showing an rms scatter of 6.7 per cent. This scatter is largely

Gaussian in nature, except for a number of notable outliers. Indeed, on close inspection we find that out of the 373 individual stellar radii measurements presented in this work, 11 disagree with the Barnes–Evans derived radii by 3σ or more. Statistically, we would not expect more than one or two measurements to lie beyond 3σ. On closer inspection, apart from HD 41004A, all of the outliers [HD 6434, HD 33283 (two discrepant measurements), HD 33564, HD 82943, HD 89744, HD 128311, HD 145675, HD 186427 and HD 216437] have other radii measurements which agree well with the Barnes–Evans derived radius. We can only surmise that these discrepant points are, therefore, due to systematics.

This leaves one final quantity, the rotation period of the star, $P_{\rm rot}$, to be determined. Unfortunately, for the reasons stated earlier, the majority of stars targeted in extra-solar planet hunts are not highly active stars. Therefore, their rotation periods generally cannot be measured by tracking of large, cool starspots on their surfaces, for example. They are often, however, sufficiently active to show Ca II H and K emission in their spectra. Noyes et al. (1984) derived the ratio, $R'_{\rm HK}$, of Ca II H and K chromospheric emission to the total bolometric emission for a number of stars whose rotation periods were known from variability in their light curves. They found that, as expected from stellar dynamo theory, the mean level of Ca II H and K emission is correlated with rotation period. In addition, the emission also depends on the spectral type (probably due to convective zone depth). Noyes et al. (1984) were then able to determine the following rotation period – activity relationship for main-sequence stars,

$$\log(P_{\rm rot}/\tau) = 0.324 - 0.400y - 0.283y^2 - 1.325y^3, \quad (6)$$

where $y = \log(10^5\ R'_{\rm HK})$. The value for the convective turnover time, τ, can be obtained from the empirical function,

$$\log\tau = \begin{cases} 1.362 - 0.166x + 0.025x^2 - 5.323x^3 & : x > 0 \\ 1.362 - 0.14x & : x < 0, \end{cases} \quad (7)$$

where $x = 1 - (B - V)$. Thus, the stellar rotation period can be determined from equation (6) if $R'_{\rm HK}$ and the $B - V$ colours are known.

We are in the fortunate position that many of the extra-solar planet hosts have published $R'_{\rm HK}$ values, since investigators generally wish to show that the host stars exhibit low-level magnetic activity and hence discard activity as the cause of radial velocity variations. Furthermore, most extra-solar planet hosts are bright stars, of which several have been observed by long-term surveys such as the Mount Wilson HK survey that started in the mid-1960s (Wilson 1978). Since the level of Ca II H and K emission may vary with time due to, for example, solar-like activity cycles or rotation of magnetic regions, $R'_{\rm HK}$ measurements need to be averaged over a suitably long (nearly a decade) baseline. Given a suitable span of observations, Noyes et al. (1984) found that they could predict the rotation periods of stars with a reasonably high accuracy. Obviously, for stars where only a few $R'_{\rm HK}$ observations have been made, the error on the rotation period may be much higher due to intrinsic variability in the Ca II H and K emission. This is discussed in Section 3.1.

3 APPLICATION TO KNOWN EXTRA-SOLAR PLANETS

In order to calculate the $\sin i$'s of the extra-solar planet hosts, we have conducted an intensive literature and data base search to determine the three quantities $v \sin i$, R_* and $\log R'_{\rm HK}$. The values we have found are presented in Table 1. Extra-solar planet host stars for which we could not find estimates of all three quantities ($v \sin i$, R_* and $\log R'_{\rm HK}$) are not presented in this table. Where identifiable, we have attempted to remove any duplicate measurements. For example, many of the $v \sin i$ measurements taken from the NASA Stellar Archive and Exoplanet Data base (NStED – see http://nsted.ipac.caltech.edu/) were found to be rounded values from Fischer & Valenti (2005) and have therefore not been included in Table 1 in these cases.

The values in Table 1 have then been used to determine $v \sin i$, R_* and $P_{\rm rot}$ for each star in our sample to obtain $\sin i$ via equation (1) as follows. We have taken a weighted mean for the final values of $v \sin i$ and R_* (the latter includes our radius estimate derived from the Barnes–Evans technique). Where no error was quoted for a value of $v \sin i$ we have taken it to be $1.0\,{\rm km\,s^{-1}}$, which is twice the typical error assumed on $v \sin i$ measurements (see the catalogue of Fischer & Valenti 2005, for example). Regarding radii with no associated error estimate, we have taken the error to be 10 or 20 per cent of the absolute value. We have chosen 10 per cent when the only radius measurement/s available for a particular star does not indicate uncertainties. Where there is more than one radius estimate for a star, of which one or more do not include error bars, then we have assumed the error bar to be either 10 or 20 per cent. We chose whether to adopt a 10 or 20 per cent uncertainty such that radii estimates with associated error bars were given a higher weighting than those without formal error bars in the final weighted mean.

3.1 Adopted $\log R'_{\rm HK}$ values and errors

The adopted values and error estimates for the $\log R'_{\rm HK}$ measurements require special mention. A comprehensive literature search has been conducted and for each $\log R'_{\rm HK}$ measurement reported in Table 1 we have determined, where possible, the number of observations and period span over which they were carried out. This detailed information is summarized in Table 2. Where details of the $\log R'_{\rm HK}$ measurements are either not present or ambiguous, we have assumed that they are from a single observation and have flagged them as *'individual?'*. Where available we have also quoted any reported variations or error estimations in either the S-index [see Wright et al. (2004) for the definition of S-index, but note that their equation (10) is in error and the left-hand side should read $\log C_{cf}(B - V) = \ldots$] or $\log R'_{\rm HK}$ measurement. These reported errors should be treated with caution since in many cases they only represent the measurement accuracy and do not sample variations in the Ca H & K emission over the course of the stellar rotation and/or activity cycle.

After establishing how well monitored each star was, they were then assigned a grade of P (Poor), O (O.K.), G (Good) or E (Excellent). A grade of 'poor' was assigned to stars with only a few individual $\log R'_{\rm HK}$ measurements which would not be sufficient to sample the variation of chromospheric emission throughout a stellar rotation. 'O' was assigned to stars with a few observations spaced over several months where the stellar rotation was probably adequately sampled, but not the activity cycle. A grade of 'good' was assigned to stars with more than 2 yr worth of observations where the stellar rotation would be well sampled, but probably only a portion of any activity cycle present had been covered. Finally, a grade of 'excellent' was assigned to objects with over a decade of $\log R'_{\rm HK}$ measurements available which covered any likely activity cycle.

Vaughan et al. (1981) present a study of chromospheric Ca H & K variations as a function of stellar rotation for 46 lower main sequence field stars. Their results show that, on average, rotation causes the modulation of the S-index (and therefore also the $\log R'_{\rm HK}$

Table 1. Published data on the properties of 154 extra-solar planet host stars. Columns 1 and 2 give the HD and HIP catalogue numbers of the host star, respectively, and Column 3 gives any other common name that the star may be known as. Published $v \sin i$ measurements and the associated error bar, σ_v, are given in Columns 4 and 5, respectively. Column 6 lists the measured $\log R'_{HK}$ found from the literature, and Columns 7 and 8 list any stellar rotation periods and corresponding errors that are quoted. Note that the stellar rotation period may not correspond to the $\log R'_{HK}$ on the same line. Actual *observed rotation periods* are indicated with an asterisk next to the measurement. The final two columns give the published values and error bars for the stellar radius. References for the values are indicated by the numbers in superscript and can be found at the end of the table. We have also included the radii we have calculated for each star from the Barnes–Evans relationship (reference number 93). Where rotation periods do not have an associated reference number, they have been calculated using the adjacent P_{rot} value and the Noyes et al. (1984) chromospheric emission–rotation period relationship along with $(B - V)$ values taken from the NStED data base. Only the first seven lines and citation list are presented here; the full version of the table is available online only (see Supporting Information).

HD	HIP	Alternative name	$v \sin i$ (km s^{-1})	σ_v	$\log R'_{HK}$	P_{rot} (d)	σ_P	R_* ($R_\odot$)	σ_R
(1)	(2)	(3)	(4)	(5)	(6)	(7)	(8)	(9)	(10)
142	522		10.350[3]	0.500	−5.020[1]	10.747	...	1.440[4]	0.070
			...	...	−4.950[92]	10.058	...	1.353[16]	0.024
			...	...	...	...	...	1.452[93]	0.034
1237	1292	GJ 3021	6.000[9]	...	−4.440[5]	10.400[5]	...	0.940[4]	0.050
			5.500[8]	...	−4.270[6]	12.600[7]	...	0.850[3]	...
			5.030[3]	...	−4.340[1]	6.549	...	0.865[65]	0.055
			...	...	...	...	...	0.902[93]	0.016

References: [1]Saffe, Gómez & Chavero (2005), [2]Butler et al. (2006), [3]Fischer & Valenti (2005), [4]NStED, [5]Barnes et al. (2001), [6]Coralie, [7]Geneva, [8]Coravel, [9]Nordström et al. (2004), [10]Moutou et al. (2005), [11]Fracassini et al. (2001), [12]Pizzolato et al. (2003), [13]Wright et al. (2004), [14]Barnes (2007), [15]California & Carnegie Planet Search Team, [16]Valenti & Fischer (2005), [17]Udry et al. (2006), [18]Mayor et al. (2004), [19]Perrier et al. (2003), [20]Fuhrmann, Pfeiffer & Bernkopf (1998), [21]Bernkopf, Fidler & Fuhrmann (2001), [22]Fischer et al. (2007), [23]Fischer et al. (2001), [24]Saar & Osten (1997), [25]Reiners & Schmitt (2003), [26]Jones et al. (2006), [27]O'Toole et al. (2007), [28]Johnson et al. (2006a), [29]Galland et al. (2005), [30]Acke & Waelkens (2004), [31]Santos et al. (2002), [32]Fischer et al. (2002), [33]Hatzes et al. (2006), [34]de Medeiros & Mayor (1999), [35]Lovis et al. (2006), [36]Lowrance et al. (2005), [37]Messina, Rodonò & Guinan (2001), [38]Henry et al. (1996), [39]Udry et al. (2003), [40]Naef et al. (2004), [41]Naef et al. (2001), [42]Sozzetti et al. (2006), [43]Bernacca & Perinotto (1970), [44]Korzennik et al. (2000), [45]Lovis et al. (2005), [46]Fuhrmann, Pfeiffer & Bernkopf (1997), [47]Naef et al. (2007), [48]Ge et al. (2006), [49]Melo et al. (2007), [50]Sato et al. (2003), [51]Fischer et al. (2006), [52]Vogt et al. (2002), [53]Udry et al. (2002), [54]Eggenberger et al. (2006), [55]Soderblom (1982), [56]Benz & Mayor (1984), [57]Bakos et al. (2007b), [58]Da Silva et al. (2006), [59]Santos et al. (2004), [60]Pepe et al. (2002), [61]Johnson et al. (2007), [62]Johnson et al. (2006b), [63]Bouchy et al. (2005), [64]Melo et al. (2006), [65]Masana, Jordi & Ribas (2006), [66]Naef et al. (2003), [67]Henry, Donahue & Baliunas (2002b), [68]Santos et al. (2000), [69]Mazeh et al. (2000) [70]Fuhrmann (1998), [71]Lo Curto et al. (2006), [72]Pepe et al. (2004), [73]Alonso et al. (2004), [74]Sozzetti et al. (2004), [75]Narita et al. (2007), [76]Laughlin et al. (2005), [77]Sozzetti et al. (2007), [78]Bakos et al. (2007a), [79]Pont et al. (2007), [80]Santos et al. (2006), [81]Queloz et al. (2000), [82]Bouchy et al. (2004), [83]Konacki et al. (2004), [84]Torres, Winn & Holman (2008), [85]Konacki et al. (2005), [86]Irwin et al. (2008), [87]Henry et al. (2002a), [88]Strassmeier et al. (2000), [89]Butler et al. (2003), [90]Butler et al. (2000), [91]Santos et al. (2001), [92]Jenkins et al. (2006), [93]Derived from the Barnes–Evans relationship of Fouque & Gieren (1997).

measurements) by 7.3 per cent for F-stars, 9.4 per cent for G-stars and 13 per cent for K-stars. We refer to these values as the *average rotationally modulated variations* or ARMV. In addition, Vaughan et al. (1981) show that modulations due to activity cycles are typically twice that caused by rotation. We have used this to assign general error bars on the $\log R'_{HK}$ values for our stars dependent upon their spectral type and assigned grades (P, O, G or E) as follows:

(i) Grade P: 2.0 × the ARMV,
(ii) Grade O: 1.5 × the ARMV,
(iii) Grade G: 1.0 × the ARMV,
(iv) Grade E: 0.5 × the ARMV.

Table 2. Compilation of chromospheric indices ($\log R'_{HK}$) for the stars in Table 1. The spectral type of the host star is given in Column 2. Entries in bold give the grade assigned to each star (P = Poor, O = O.K., G = Good and E = Excellent) followed by the weighted mean of the $\log R'_{HK}$ measurements and adopted error bar (see Section 3.1 for details). Reference numbers are identical to those used in Table 1. Only the first seven lines are presented here; the full version of the table is available online only (see Supporting Information).

Name	Type	log R'$_{HK}$	Observations	Ref.
HD 142	F7	−5.020	Average of two individual points	1
		−4.950	Individual on 2001 Aug 04	92
			(P) Adopted value: -4.997 ± 0.060	
HD 1237	G6	−4.440	1992 individual	5
		−4.270	61 obs in 2 years	6
		−4.340	Average of above + extra individual	1
			(G) Adopted value: -4.273 ± 0.170	

Thus, stars with only a few individual observations are assigned an error that would cover the entire range in Ca H & K variations seen over a typical activity cycle. The error bars assigned to the other categories are somewhat ad hoc, but signify an improvement in the reliability of the average $\log R'_{\rm HK}$ as the sampling of the activity cycle is improved. Given the amalgamation of sources for the $\log R'_{\rm HK}$ observations, we feel this is as robust an error treatment that the data can be given in most cases. For objects with several independent $\log R'_{\rm HK}$ measurements, this error assignment generally covers the observed variations well. In the few cases where they do not, we have expanded the error bar to cover the observed $\log R'_{\rm HK}$ variations appropriately. Finally, for objects whose activity cycles have been well monitored and for which we can define a maximum variation across the cycle, we have taken these limits as representing the 3σ variation on the average $\log R'_{\rm HK}$ value. (For example, if a well-sampled star has a mean $\log R'_{\rm HK} = -4.9$ but varies from -4.8 to -5.0, we assigned a 1σ error $= 0.1/3$.)

Where two or more $\log R'_{\rm HK}$ measurements are available we have taken a weighted mean of their values. The weightings are based on either how many observations have been taken or the time-span over which the observations were taken, depending on what information exists. We have then calculated the stellar rotational period using the Noyes et al. (1984) relationship and $B - V$ values from the NStED data base. The rotation periods and the associated error bars we have calculated are presented in Tables 3 and 4 and can be compared to the rotation periods obtained in the literature shown in Table 1. Note, however, that we found several cases where authors have clearly calculated the rotation period from $\log R'_{\rm HK}$ incorrectly (see Appendices A and B).

4 MARKOV-CHAIN MONTE CARLO ANALYSIS

Equation (1) can be thought of as a naive estimator of $\sin i$. By simply inputting the derived values for $v \sin i, R_*$ and $P_{\rm rot}$ for each host star (as discussed earlier), it is possible to obtain an unconstrained distribution of $\sin i$ values (i.e. values of $\sin i > 1$ are possible). Due to uncertainties in $v \sin i, R_*$ and $P_{\rm rot}$, this naive estimator will, however, occasionally yield unphysical $\sin i$ values greater than 1. Table 3 lists all the exoplanet host stars which yield a $\sin i > 1$ as calculated from equation (1), along with their formal error bars.

For the purposes of this paper, however, we wished to carry out a Markov-chain Monte Carlo (MCMC) analysis on the extra-solar planet host stars. MCMC has the major advantage over simply using our naive estimator (equation 1) in that, not only does it provide a means of optimizing the fit of a model to data, but it also explores the joint posterior probability distribution of the fitted parameters. This means that proper 1σ two-tailed confidence limits can be placed on the derived $\sin i$'s, as well as allowing the probability of a transit being observed to be calculated from purely spectroscopic data. MCMC has been used in several areas of astronomy, and instead of outlining in detail its operation here, we refer the readers to Tegmark et al. (2004), Ford (2006) and Gregory (2007), who have applied MCMC to various astronomical problems including deriving cosmological parameters from the cosmic microwave background, and deriving physical parameters of extra-solar planet systems. In particular, our version of MCMC is modified from the code used by Collier Cameron et al. (2007) to identify extra-solar planet transit candidates.

Naturally, values of $\sin i > 1$ are unphysical, and the MCMC rejects those combinations of parameters that result in $\sin i > 1$. If, however, we imagine the hypothetical case where we have a population of transiting extra-solar planets all with $\sin i = 1$ then, due to measurement errors, on average half of these systems would yield $\sin i > 1$ from equation (1). Obviously, we would not want to reject these systems on this basis, since they do not contradict our null hypothesis that the measurements are free from systematic errors. One particular example of this is HD 209458, which is a known transiting planet and yields $\sin i = 1.096 \pm 0.108$ from our naive estimator, equation (1) (see Table 3). We do, however, want to reject those systems where it is likely that there are systematic errors in their R_*, $P_{\rm rot}$ and $v \sin i$ measurements leading to $\sin i > 1$. We have, therefore, included all systems from Table 3 which are within 1σ of $\sin i = 1$ in our MCMC analysis and have error bars <0.5.

For the purposes of this paper, we feed the MCMC with the measured values of $R_*, P_{\rm rot}, v \sin i$ and their associated error bars, $\sigma_{\rm R}, \sigma_{\rm P}, \sigma_{\rm v}$, respectively. We assume that the stellar inclinations are randomly distributed and hence follow a uniform distribution with $0 < x < 1$, where $x = \cos i$. For the purposes of calculating the transit probabilities of the extra-solar planets, we have also assumed that the stellar mass follows the mass–radius relationship $M_* = R_*^{1.25}$ (Tingley & Sackett 2005).

The three quantities, $R_*, P_{\rm rot}$ and x, constitute the 'proposal parameters' with analogy to the description of the implementation of MCMC outlined by Collier Cameron et al. (2007). We can then perform a random walk through parameter space by perturbing each proposal parameter from its previous value by a random amount:

$$\begin{aligned} R_{*,i} &= R_{*,i-1} + G\sigma_{\rm R} \\ P_{{\rm rot},i} &= P_{{\rm rot,i}-1} + G\sigma_{\rm P} \\ x_i &= x_{i-1} + G\sigma_x, \end{aligned}$$

where G is a Gaussian random number with zero mean and unit variance. The initial value of $x = \cos i$ was set to 0.5 and given an arbitrary standard deviation $\sigma_x = 0.05$ which was later re-evaluated empirically from the Markov chains themselves (see later).

After each perturbation, χ^2 was evaluated for the new set of proposal parameters via

$$\chi_i^2 = \frac{(R_{*,i} - R_{*,0})^2}{\sigma_{\rm R}^2} + \frac{(P_{{\rm rot},i} - P_{{\rm rot},0})^2}{\sigma_{\rm P}^2} + \frac{(2\pi R_{*,i}\sqrt{\left[1 - x_i^2\right]}/P_{\rm rot,i} - v \sin i)^2}{\sigma_{\rm v}^2}, \quad (8)$$

where $\sqrt{\left[1 - x_i^2\right]} = \sin i$, $v \sin i$ is the measured projected stellar rotation velocity and $R_{*,0}$, $P_{{\rm rot},0}$ are the measured stellar radius and rotation period, respectively. For each jump, if $\chi_i^2 < \chi_{i-1}^2$ then the new parameters were accepted, otherwise the new parameters were accepted with the acceptance probability given by $\exp[-(\chi_i^2 - \chi_{i-1}^2)/2]$ (the Metropolis–Hastings rule). The uncertainty σ_x was recomputed from the Markov chains themselves every 100 successful steps by calculating the standard deviation on x over these 100 jumps.

We found that it was necessary to carry out 1000 000 jumps in order for the MCMC to return the maximum-likelihood value of $\sin i$ that accurately approached the value obtained from equation (1). The Markov chains were then evaluated (after discarding a 1000-step long burn-in phase) in order to determine the 1σ two-tailed confidence limits on $\sin i$. In addition, for each set of new parameters generated within the Markov chain, we evaluated whether or not the extra-solar planet (or extra-solar planets in the case of multiple systems) would transit the host star. Thus, our implementation of MCMC also returns the transit probability for each extra-solar planet in the study. We should note, however, that we have assumed that the extra-solar planets follow circular orbits, so our calculated transit

Table 3. Adopted parameters and $\sin i$ estimates for all extra-solar planet host stars with $\sin i > 1$ as derived from equation (1). The first three columns are as described in Table 1. Sub-giants are indicated with an asterisk as they may not follow the rotation period–activity relationship of Noyes et al. (1984). Column 4 lists the stellar rotation period (in d) obtained from the measured $\log R'_{\rm HK}$'s listed in Table 1, and Column 5 gives the error bar adopted from the scatter measured for the Ca II H & K emission–rotation period relationship of Noyes et al. (1984). Columns 6 and 7 give the radii and associated error bar adopted from Table 1. See Section 3 for an in-depth discussion of how the adopted values were obtained. The final two columns give the resulting $\sin i$ value and corresponding error bar which have been calculated using equation (1) and a formal error propagation. Sub-giants are indicated with an asterisk.

HD or alt. name (1)	$v \sin i$ (km s^{-1}) (2)	$\sigma_{\rm v}$ (3)	$P_{\rm rot}$ (d) (4)	$\sigma_{\rm P}$ (5)	R_* ($R_\odot$) (6)	$\sigma_{\rm R}$ (7)	$\sin i$ (8)	$\pm$ (9)
142*	10.349	0.500	10.524	0.599	1.389	0.018	1.548	0.117
2039*	3.250	0.500	25.487	2.34	1.256	0.097	1.302	0.247
3651	1.149	0.500	44.000	9.793	0.878	0.008	1.137	0.555
8574	4.327	0.386	17.073	0.884	1.383	0.029	1.054	0.111
9826	9.482	0.362	11.910	1.18	1.586	0.017	1.406	0.132
11506	5.000	0.447	18.300	0.696	1.397	0.046	1.293	0.132
11964*	2.700	0.500	50.492	2.553	2.032	0.045	1.325	0.256
13445	2.259	0.179	27.240	6.203	0.823	0.003	1.477	0.356
19994	8.511	0.408	10.783	1.682	1.698	0.028	1.067	0.175
23127	3.299	0.500	32.034	2.285	1.574	0.071	1.326	0.230
23596	3.956	0.381	21.251	1.108	1.583	0.048	1.049	0.119
27442*	2.873	0.257	89.184	15.674	4.335	0.427	1.167	0.257
27894	1.500	1.000	44.449	4.177	0.844	0.031	1.559	1.051
28185	2.484	0.461	29.976	2.685	1.062	0.031	1.384	0.288
30177	2.959	0.500	45.399	2.896	1.152	0.028	2.303	0.419
33283	3.360	0.447	58.678	6.985	1.306	0.049	2.981	0.544
33564	12.390	0.937	6.802	0.429	1.503	0.024	1.107	0.110
33636	3.080	0.500	16.697	0.966	1.003	0.022	1.012	0.176
38529	3.899	0.500	37.761	2.210	2.750	0.079	1.057	0.152
50499	4.209	0.500	22.160	1.146	1.428	0.027	1.289	0.168
52265	4.775	0.447	15.791	1.191	1.275	0.022	1.168	0.142
63454	1.899	1.000	20.251	5.316	0.744	0.024	1.021	0.601
68988	2.839	0.500	26.459	0.926	1.182	0.037	1.255	0.228
73526	2.620	0.500	35.643	2.433	1.505	0.077	1.225	0.256
75289	4.139	0.500	16.839	1.201	1.271	0.016	1.083	0.152
75732	2.467	0.447	46.791	3.800	0.953	0.009	2.392	0.475
80606	1.431	0.384	42.254	2.62	0.941	0.192	1.268	0.432
86081	4.200	0.500	24.838	1.683	1.295	0.079	1.590	0.238
88133*	2.185	0.353	49.838	3.263	2.080	0.113	1.033	0.189
99109*	1.891	0.447	48.485	3.252	1.081	0.048	1.675	0.418
99492	1.379	0.353	46.585	3.923	0.789	0.031	1.609	0.438
100777	1.800	1.000	40.084	1.433	1.133	0.061	1.258	0.703
102195	3.226	0.069	18.429	10.979	0.835	0.013	1.405	0.838
108874	2.220	0.500	40.610	1.401	1.246	0.070	1.429	0.335
109749	2.399	0.447	27.091	1.810	1.243	0.075	1.032	0.213
111232	2.600	1.000	30.437	2.263	0.899	0.017	1.737	0.681
117176	2.827	0.249	35.463	3.4	1.825	0.025	1.085	0.133
128311	3.649	0.500	10.778	2.714	0.769	0.011	1.009	0.289
130322	1.667	0.447	29.377	19.924	0.824	0.026	1.173	0.856
134987	2.169	0.500	33.778	1.649	1.225	0.018	1.181	0.278
142022A	2.100	1.000	42.052	2.368	1.085	0.028	1.607	0.772
145675	1.560	0.500	48.500	1.137	0.984	0.009	1.519	0.488
149143*	3.979	0.447	26.703	2.31	1.487	0.055	1.411	0.198
160691	3.662	0.182	32.157	2.172	1.322	0.018	1.758	0.149
164922	1.808	0.447	44.192	1.547	0.980	0.013	1.610	0.402
168443	2.100	0.447	38.606	0.675	1.595	0.030	1.004	0.215
177830*	2.540	0.500	65.711	6.921	3.129	0.105	1.053	0.237
178911B	1.939	0.500	36.250	2.24	1.130	0.183	1.229	0.381
185269*	5.679	0.447	21.458	1.382	1.890	0.054	1.273	0.134
186427	2.253	0.315	29.343	0.767	1.167	0.009	1.119	0.159
187085	5.099	0.500	14.349	1.206	1.331	0.045	1.085	0.145
190360	2.320	0.447	35.807	0.621	1.151	0.013	1.425	0.276
190647	1.969	0.832	40.977	1.410	1.496	0.061	1.065	0.453

Table 3 – *continued*

HD or alt. name (1)	$v \sin i$ (km s^{-1}) (2)	$\sigma_{\rm v}$ (3)	$P_{\rm rot}$ (d) (4)	$\sigma_{\rm P}$ (5)	R_* ($R_\odot$) (6)	$\sigma_{\rm R}$ (7)	$\sin i$ (8)	$\pm$ (9)
192263	2.501	0.447	20.773	12.259	0.775	0.014	1.324	0.817
196050	3.235	0.447	23.282	7.293	1.321	0.039	1.126	0.387
196885*	7.750	0.500	12.306	0.672	1.387	0.027	1.358	0.117
209458	4.280	0.367	14.914	0.629	1.150	0.029	1.096	0.108
210277	1.839	0.447	40.141	1.849	1.081	0.012	1.349	0.334
212301	6.220	1.000	11.340	0.492	1.172	0.030	1.188	0.200
216435*	5.780	0.500	21.299	1.567	1.768	0.031	1.375	0.158
216437*	3.004	0.447	26.985	1.857	1.470	0.019	1.088	0.179
216770	1.813	1.000	38.656	5.99	0.997	0.027	1.388	0.788
217014	2.178	0.367	29.467	0.766	1.159	0.010	1.093	0.187
219828	3.450	1.000	28.476	1.439	1.842	0.128	1.053	0.318
222582	2.290	0.500	25.032	1.786	1.128	0.030	1.003	0.232
224693*	3.799	0.447	29.735	1.487	1.831	0.148	1.218	0.184
OGLE-TR-56	3.200	1.000	26.312	2.204	1.234	0.042	1.347	0.438
OGLE-TR-111	5.000	1.000	37.964	6.118	0.829	0.020	4.518	1.165

probabilities may not be accurate for extra-solar planets with highly eccentric orbits. Furthermore, objects are flagged as transiting if the planets centre crosses the stellar disc – the planetary radius is not taken into account. The results of the MCMC analysis are shown in Table 4.

5 POSSIBLE SOURCES OF SYSTEMATIC ERRORS

While we have already highlighted possible sources of error arising from, for example, variation of the chromospheric emission due to rotation of active regions or stellar activity cycles, it is pertinent to look into other possible sources of systematics. These include potential biases as a result of differing line-of-sight effects, our use of an inhomogeneous set of data from a number of different studies, selection effects and problems arising due to our ignorance of the physics at work that affect the measurables in equation (1). We shall discuss possible systematics affecting the estimation of the parameters in the right-hand side of equation (1) (namely $P_{\rm rot}$, $v \sin i$ and R_*) in turn.

5.1 Systematic errors on $P_{\rm rot}$

Most of the stellar rotation periods reported in this paper have been estimated from the strength of the chromospheric Ca II H & K emission with the exception of a few that have been determined photometrically. Rotation periods calculated from the analysis of Ca II H & K emission are, as previously described in detail in Section 3.1, impacted by variability caused by activity cycles and the temporal evolution of magnetic regions. On top of this, however, there may also be line-of-sight geometry effects to consider for given starspot or active region distributions. For instance, Doppler images of rapidly rotating active stars (e.g. Cameron & Donati 2002; Watson, Dhillon & Shabaz 2006; Watson et al. 2007; Skelly et al. 2009) have revealed the presence of high-latitude and even polar spots covering a significant fraction of the stellar surface. This is in stark contrast to our Sun where spots are rarely observed at latitudes $>40^\circ$ and seldomly cover more than $\sim$1 per cent of the solar surface.

Assuming that the bulk Ca II H & K emission arises from regions associated with starspots, then the distribution of spots coupled with the inclination of the stellar rotation axis to the observers line-of-sight could systematically affect the derived rotation period. For example, consider a star with a large polar active region. In this case the observer would see a larger projected area of activity when viewed at a low inclination (from above the pole) compared to the same distribution viewed edge-on at high inclinations. Under this scenario this would lead to seemingly higher levels of chromospheric activity observed in rapidly rotating stars viewed at low inclinations. This, in turn, would lead to systematically shorter $P_{\rm rot}$ estimates for rapidly rotating, low inclination stars and (from equation 1) drive the estimated $\sin i$ to even lower values. Conversely, rapidly rotating stars viewed at high inclinations would, presumably, have $\sin i$ estimates systematically biased towards higher values. Unfortunately, we are largely ignorant of the exact interplay between spot numbers, sizes and distributions and the corresponding Ca II H & K emission which makes the estimation of the magnitude of this effect beyond the scope of this paper. This is further exasperated by our lack of detailed understanding of how stellar activity varies as a function of spectral-type and stellar age (or, equivalently, rotation rate).

In addition, the majority of exoplanet host stars are, by selection, relatively inactive and therefore exhibit low Ca II H & K emission. For these stars, there may be a possible bias towards measurements of higher $R'_{\rm HK}$ values, since it should be easier to detect their Ca II H & K emission at the peak of their activity. This would cause the estimated stellar rotation rates to be too fast, skewing our $\sin i$ distribution to low values.

5.2 Systematic errors on derived $v \sin i$'s

The $v \sin i$ values quoted in this work come from a variety of sources and are not from a homogeneous sample. For many exoplanet discovery papers the value of the rotational broadening of the host star is often reported with little discussion as to how this was determined. This is of little surprise, since the authors are largely preoccupied with characterizing the planet rather than the parent star. However, it raises the question of whether the reported $v \sin i$ values are accurate and, in addition, also correct relative to one another.

The observed stellar line broadening is a function of the intrinsic line-profile width, convolved with the rotationally broadened profile and the instrumental profile. Thus, to the first approximation the

Table 4. Adopted parameters and $\sin i$ estimates for extra-solar planet host stars for which we have carried out an MCMC analysis. Extra-solar planets with $\sin i$ values more than 1σ greater than 1 (see Table 3) were excluded from this analysis. Columns 1–7 are described in Table 3. For stars with multiple planets, the first row gives the full planet name, and subsequent planets are indicated in the following rows by their designated letter only (e.g. 'c', 'd', etc.). Sub-giants are indicated with an asterisk. Column 8 lists the calculated $\sin i$'s for each star given the adopted $v \sin i$, $P_{\rm rot}$ and R_*, and Columns 9 and 10 list the two-tailed 1σ error bars on $\sin i$. Column 11 lists the exoplanet mass (in Jupiter masses) after applying the $\sin i$ correction in Column 8. Finally, Column 12 gives the transit probability for each extra-solar planet, where 1 indicates a 100 per cent probability that the system shows transits.

HD or alt. name (1)	$v \sin i$ (km s^{-1}) (2)	$\sigma_{\rm v}$ (3)	$P_{\rm rot}$ (d) (4)	$\sigma_{\rm P}$ (5)	R_* ($R_\odot$) (6)	$\sigma_{\rm R}$ (7)	$\sin i$ (8)	σ_- (9)	σ_+ (10)	Mass ($M_{\rm J}$) (11)	prob. (12)
1237	5.510	1.000	4.314	3.213	0.901	0.014	0.527	0.365	0.413	6.295	0.004
2638	1.100	1.000	38.832	4.626	0.926	0.057	0.905	0.153	0.094	0.530	0.055
4203	1.229	0.500	43.015	1.550	1.403	0.075	0.744	0.211	0.213	2.215	0.002
4308	0.400	0.447	22.524	2.12	1.029	0.009	0.174	0.172	0.306	0.269	0.000
6434	2.149	1.000	17.235	1.620	0.910	0.031	0.811	0.176	0.166	0.591	0.013
8574	4.327	0.386	17.073	0.884	1.383	0.029	0.999	0.049	0.000	2.230	0.009
10647	5.464	0.447	7.669	1.38	1.101	0.014	0.756	0.155	0.160	1.203	0.001
10697	2.479	0.500	34.273	1.181	1.791	0.032	0.941	0.069	0.058	6.502	0.002
12661	1.300	0.500	37.253	2.457	1.145	0.025	0.834	0.142	0.151	2.755	0.003
c	.	.	.	.	.	.	.	.	.	1.881	0.001
16141	1.743	0.447	31.839	1.554	1.453	0.043	0.754	0.187	0.194	0.305	0.006
17051	5.599	0.304	7.921	1.626	1.156	0.012	0.756	0.180	0.191	2.565	0.002
17156	2.600	0.500	22.138	1.118	1.504	0.056	0.754	0.165	0.177	4.123	0.011
19994	8.511	0.408	10.783	1.682	1.698	0.028	0.999	0.066	0.000	2.001	0.006
20367	3.290	1.000	5.465	1.497	1.200	0.025	0.293	0.135	0.184	3.650	0.000
20782	2.391	0.447	20.462	1.980	1.124	0.021	0.864	0.118	0.118	2.083	0.002
22049	1.898	0.257	11.679	6.801	0.721	0.007	0.588	0.295	0.359	2.632	0.001
23079	2.990	0.500	17.117	1.182	1.128	0.014	0.895	0.091	0.094	2.914	0.002
23596	3.956	0.381	21.251	1.108	1.583	0.048	0.999	0.055	0.000	7.191	0.003
27442*	2.873	0.257	89.184	15.674	4.335	0.427	0.999	0.080	0.000	1.280	0.010
33564	12.390	0.937	6.802	0.429	1.503	0.024	0.999	0.037	0.000	9.100	0.008
33636	3.080	0.500	16.697	0.966	1.003	0.022	0.999	0.094	0.000	9.282	0.001
37124	1.219	0.500	27.311	0.650	1.006	0.027	0.645	0.258	0.278	0.946	0.003
c	.	.	.	.	.	.	.	.	.	1.059	0.000
d	.	.	.	.	.	.	.	.	.	0.930	0.001
38529	3.899	0.500	37.761	2.210	2.750	0.079	0.999	0.068	0.000	0.780	0.079
c	.	.	.	.	.	.	.	.	.	12.705	0.002
39091	3.140	0.500	17.328	1.583	1.161	0.010	0.924	0.067	0.074	11.193	0.001
40979	7.429	0.500	7.896	0.948	1.205	0.020	0.964	0.047	0.035	3.443	0.005
41004A	1.609	1.000	26.897	6.627	1.016	0.045	0.833	0.136	0.160	2.759	0.001
45350	1.370	0.500	39.402	1.921	1.299	0.035	0.818	0.155	0.160	2.187	0.001
46375	0.859	0.500	43.876	3.514	1.024	0.027	0.738	0.233	0.223	0.337	0.058
49674	0.419	0.500	27.226	1.740	0.974	0.025	0.241	0.239	0.467	0.477	0.007
50554	3.675	0.356	14.665	0.474	1.134	0.021	0.939	0.056	0.056	5.217	0.002
62509	1.331	0.668	135.000	13.500	8.738	0.098	0.392	0.329	0.523	7.393	0.004
69830	0.700	0.353	36.452	1.929	0.892	0.010	0.554	0.311	0.339	0.060	0.015
c	.	.	.	.	.	.	.	.	.	0.069	0.006
d	.	.	.	.	.	.	.	.	.	0.105	0.002
70573	12.300	1.000	3.295	31.226	0.846	0.251	0.991	0.244	0.000	6.155	0.002
70642	0.299	0.500	28.829	3.276	1.016	0.013	0.167	0.166	0.520	11.932	0.000
72659	2.209	0.500	20.731	0.759	1.458	0.043	0.616	0.177	0.191	4.798	0.000
73256	3.260	1.000	13.912	3.897	0.966	0.025	0.921	0.113	0.078	2.029	0.077
73526	2.620	0.500	35.643	2.433	1.505	0.077	0.999	0.083	0.000	2.900	0.009
c	.	.	.	.	.	.	.	.	.	2.500	0.005
74156	4.217	0.389	18.202	0.891	1.627	0.063	0.935	0.061	0.059	2.011	0.016
c	.	.	.	.	.	.	.	.	.	8.588	0.001
d	.	.	.	.	.	.	.	.	.	0.424	0.004
75289	4.139	0.500	16.839	1.201	1.271	0.016	0.999	0.063	0.000	0.410	0.148
76700	1.350	0.500	36.599	4.721	1.372	0.031	0.709	0.215	0.238	0.277	0.049
80606	1.431	0.384	42.254	2.62	0.941	0.192	0.999	0.128	0.000	3.410	0.008
81040	2.000	1.000	9.085	2.12	0.887	0.033	0.400	0.290	0.368	17.136	0.000
82943	1.420	0.447	21.892	1.912	1.098	0.018	0.566	0.250	0.254	3.090	0.001
c	.	.	.	.	.	.	.	.	.	3.550	0.001
83443	1.303	0.447	35.999	4.37	1.058	0.024	0.868	0.105	0.127	0.460	0.069
88133*	2.185	0.353	49.838	3.263	2.080	0.113	0.999	0.093	0.000	0.220	0.166

Table 4 – *continued*

HD or alt. name (1)	$v \sin i$ (km s^{-1}) (2)	$\sigma_{\rm v}$ (3)	$P_{\rm rot}$ (d) (4)	$\sigma_{\rm P}$ (5)	R_* ($R_\odot$) (6)	$\sigma_{\rm R}$ (7)	$\sin i$ (8)	σ_- (9)	σ_+ (10)	Mass ($M_{\rm J}$) (11)	prob. (12)
89307	2.879	0.500	17.155	1.369	1.075	0.024	0.909	0.086	0.084	3.001	0.001
89744	9.208	0.447	9.000	6.785	2.126	0.041	0.763	0.191	0.212	10.461	0.006
92788	0.567	0.447	33.611	1.702	1.049	0.020	0.375	0.369	0.427	10.276	0.001
93083	0.900	1.000	48.549	3.434	0.874	0.026	0.990	0.233	0.009	0.374	0.004
95128	2.830	0.231	21.113	0.373	1.220	0.012	0.969	0.033	0.030	2.681	0.002
c	.	.	.	.	.	.	.	.	.	0.474	0.002
101930	0.699	1.000	46.575	3.485	0.907	0.028	0.710	0.238	0.253	0.422	0.007
102117	1.004	0.447	37.555	1.342	1.314	0.026	0.580	0.320	0.298	0.296	0.009
104985	2.699	1.100	120.982	29.627	10.273	1.176	0.635	0.256	0.299	9.913	0.010
106252	1.778	0.223	20.523	0.812	1.107	0.022	0.647	0.092	0.102	10.517	0.000
107148	0.705	0.447	32.451	1.660	1.186	0.034	0.385	0.369	0.371	0.545	0.002
108147	5.939	0.447	8.867	1.267	1.220	0.019	0.855	0.117	0.117	0.468	0.032
109749	2.399	0.447	27.091	1.810	1.243	0.075	0.999	0.103	0.000	0.280	0.077
114386	0.589	0.500	35.568	3.658	0.778	0.021	0.545	0.380	0.375	1.815	0.001
114729	2.290	0.500	18.836	0.333	1.439	0.029	0.590	0.161	0.166	1.389	0.000
114783	0.869	0.500	45.202	2.447	0.807	0.011	0.968	0.181	0.031	1.022	0.002
117176	2.827	0.249	35.463	3.4	1.825	0.025	0.999	0.052	0.000	7.440	0.017
117207	1.050	0.500	37.238	1.296	1.128	0.024	0.687	0.260	0.259	2.997	0.001
120136	14.735	0.173	4.000	0.400	1.426	0.016	0.777	0.020	0.221	5.015	0.109
121504	3.299	1.000	11.397	2.162	1.196	0.045	0.626	0.245	0.282	1.421	0.004
125612	2.680	0.447	17.625	0.965	1.030	0.040	0.911	0.091	0.082	3.510	0.002
128311	3.649	0.500	10.778	2.714	0.769	0.011	0.999	0.127	0.000	2.180	0.002
c	.	.	.	.	.	.	.	.	.	3.210	0.002
134987	2.169	0.500	33.778	1.649	1.225	0.018	0.999	0.106	0.000	1.580	0.005
136118	7.330	0.500	9.845	1.148	1.744	0.044	0.818	0.125	0.131	14.536	0.001
141937	1.923	0.447	15.533	2.300	1.079	0.036	0.550	0.201	0.233	17.636	0.000
142415	3.403	0.447	12.344	2.567	1.039	0.022	0.806	0.159	0.158	2.010	0.002
143761	1.420	0.300	17.000	7.223	1.328	0.015	0.350	0.232	0.331	2.969	0.001
145675	1.560	0.500	48.500	1.137	0.984	0.009	0.999	0.138	0.000	4.640	0.001
147506	19.800	1.600	4.045	0.373	1.600	0.117	0.989	0.069	0.010	8.709	0.104
147513	1.475	0.353	8.525	2.233	0.947	0.011	0.259	0.099	0.130	3.849	0.000
150706	3.650	0.325	9.428	2.195	0.959	0.012	0.691	0.191	0.242	1.446	0.002
154857	1.439	0.500	31.520	2.162	2.466	0.101	0.358	0.140	0.157	5.023	0.000
159868	2.100	0.500	35.537	2.426	1.888	0.072	0.775	0.165	0.181	2.191	0.001
162020	2.235	0.447	1.620	1.27	0.746	0.025	0.093	0.080	0.112	147.849	0.000
168443	2.100	0.447	38.606	0.675	1.595	0.030	0.999	0.117	0.000	8.021	0.016
c	.	.	.	.	.	.	.	.	.	18.101	0.002
168746	0.500	0.408	34.774	1.738	1.132	0.027	0.294	0.287	0.391	0.780	0.004
169830	3.724	0.447	9.625	1.810	1.838	0.036	0.384	0.089	0.102	7.497	0.000
c	.	.	.	.	.	.	.	.	.	10.517	0.000
170469	1.699	0.500	31.518	1.86	1.302	0.042	0.821	0.165	0.152	0.815	0.001
175541	2.899	0.500	58.171	1.324	3.800	0.008	0.880	0.109	0.102	0.693	0.006
177830*	2.540	0.500	65.711	6.921	3.129	0.105	0.999	0.111	0.000	1.280	0.006
178911B	1.939	0.500	36.250	2.24	1.130	0.183	0.999	0.126	0.000	6.294	0.012
179949	7.019	0.500	7.700	0.486	1.227	0.020	0.868	0.088	0.097	1.094	0.065
183263	1.560	0.500	28.001	1.367	1.236	0.046	0.695	0.222	0.235	5.302	0.001
186427	2.253	0.315	29.343	0.767	1.167	0.009	0.999	0.063	0.000	1.680	0.003
187085	5.099	0.500	14.349	1.206	1.331	0.045	0.999	0.057	0.000	0.750	0.003
187123	2.149	0.500	26.804	1.375	1.185	0.023	0.962	0.098	0.037	0.540	0.095
c	.	.	.	.	.	.	.	.	.	2.025	0.001
189733	2.730	0.832	13.230	5.338	0.760	0.011	0.938	0.131	0.061	1.226	0.075
190228	1.850	0.500	47.970	3.216	2.473	0.083	0.708	0.211	0.221	7.047	0.001
190647	1.969	0.832	40.977	1.410	1.496	0.061	0.999	0.180	0.000	1.900	0.002
192699	1.899	0.500	59.813	2.888	3.923	0.058	0.574	0.186	0.185	4.351	0.000
195019	2.470	0.500	29.074	2.488	1.464	0.035	0.969	0.096	0.030	3.818	0.029
196050	3.235	0.447	23.282	7.293	1.321	0.039	0.999	0.120	0.000	3.001	0.002
196885*	7.750	0.500	12.306	0.672	1.387	0.027	0.999	0.017	0.000	2.960	0.005
202206	2.299	0.500	22.980	3.585	1.064	0.032	0.984	0.125	0.015	17.674	0.004
c	.	.	.	.	.	.	.	.	.	2.478	0.001
208487	4.610	0.500	12.412	1.134	1.150	0.035	0.983	0.069	0.016	0.457	0.009
209458	4.280	0.367	14.914	0.629	1.150	0.029	0.999	0.040	0.000	0.690	0.186

Table 4 – *continued*

HD or alt. name (1)	$v \sin i$ (km s^{-1}) (2)	$\sigma_{\rm v}$ (3)	$P_{\rm rot}$ (d) (4)	$\sigma_{\rm P}$ (5)	R_* ($R_\odot$) (6)	$\sigma_{\rm R}$ (7)	$\sin i$ (8)	σ_- (9)	σ_+ (10)	Mass ($M_{\rm J}$) (11)	prob. (12)
210702	1.699	0.500	69.061	5.140	4.449	0.069	0.527	0.216	0.215	3.793	0.000
212301	6.220	1.000	11.340	0.492	1.172	0.030	0.999	0.067	0.000	0.450	0.182
213240	3.969	0.609	17.022	4.748	1.536	0.036	0.867	0.110	0.122	5.185	0.002
216437*	3.004	0.447	26.985	1.857	1.470	0.019	0.999	0.077	0.000	2.100	0.002
217014	2.178	0.367	29.467	0.766	1.159	0.010	0.999	0.081	0.000	0.468	0.106
219828	3.450	1.000	28.476	1.439	1.842	0.128	0.999	0.145	0.000	0.066	0.110
221287	5.607	0.832	4.586	0.424	1.126	0.033	0.452	0.085	0.090	6.830	0.000
222404	1.500	1.000	68.020	4.626	4.511	0.527	0.454	0.394	0.411	3.522	0.001
222582	2.290	0.500	25.032	1.786	1.128	0.030	0.996	0.119	0.003	5.129	0.003
231701	4.000	0.500	10.276	0.383	1.372	0.131	0.594	0.112	0.124	2.995	0.000
330075	0.699	0.200	47.365	3.209	1.008	0.062	0.649	0.231	0.250	1.171	0.028
TrES-1	1.195	0.169	33.528	5.968	0.824	0.015	0.970	0.091	0.029	0.629	0.081
TrES-2	2.000	1.000	24.783	1.622	1.000	0.035	0.986	0.188	0.013	1.214	0.081
HAT-P-1	2.200	0.200	19.711	1.44	1.149	0.100	0.747	0.123	0.141	0.701	0.014
OGLE-TR-10	3.000	2.000	15.836	1.925	1.143	0.042	0.809	0.154	0.178	0.778	0.068
OGLE-TR-56	3.200	1.000	26.312	2.204	1.234	0.042	0.999	0.136	0.000	1.290	0.218
OGLE-TR-113	9.000	3.000	3.244	0.748	0.765	0.025	0.763	0.191	0.201	1.730	0.082

observed line-profile full-width at half maximum ($\Delta_{\rm obs}$) is given by

$$\Delta_{\rm obs} = \sqrt{(\alpha \times v \sin i)^2 + \xi^2 + \Delta_{\rm inst}^2}, \quad (9)$$

where α is an arbitrary scaling constant to convert $v \sin i$ to a full-width half maximum, ξ is the intrinsic line-profile full-width half maximum and $\Delta_{\rm inst}$ is the instrumental profile. If the instrumental profile and/or intrinsic line-profile are ignored then the derived $v \sin i$ will be an overestimate. This would drive the $\sin i$ distribution towards high values. Furthermore, this systematic bias would be more profound for slow rotators and also for systems seen at low inclinations. If the intrinsic line-profile, ξ, is not properly treated in the estimation of $v \sin i$ then, since hotter stars have broader intrinsic line-profile widths, the problem will also become progressively worse for earlier spectral-type stars. Clearly many of these potential systematic biases could be alleviated if the data were taken from a homogeneous set and analysed in a consistent manner.

5.3 Errors on R_*

Most of the stellar radii presented in this work have been calculated by comparison of theoretical stellar atmosphere models to observed high-resolution spectra. As outlined by Brown (2010), this yields small formal errors on the radius (often better than 2 per cent), but is heavily model dependent. Brown (2010) compared the results of this technique with a group of well-calibrated eclipsing binaries, as well as single stars for which good fundamental parameters were known from asteroseismology investigations. While the results of the models compare accurately with the slowly rotating, inactive, single stars in the asteroseismic sample, a discrepancy occurs when applied to the stellar components in the eclipsing binary sample. Indeed, for this sample a mass-dependent underestimate of the stellar radius by ∼4 per cent for low-mass stars and which gradually decreased, becoming negligible for stars with masses above ∼1.4 $M_\odot$, was found.

The explanation for this underestimation is that the more rapidly rotating active stars have their radii inflated due to blocking of energy transport in the outer convection regions by star spots. Since spots do not affect the core luminosity, the stars' response to the appearance of spots is to inflate the stellar radius and/or increase the temperature of the non-spotted regions in the photosphere. Thus, more rapidly rotating stars in our sample are likely to have their radii underestimated, leading to a skew to high $\sin i$'s. Given that most of exoplanet host stars are (by selection) slowly rotating, we do not expect this to be a dominant source of systematic error. There are, however, a few cases where stars have several radii estimates available in the literature from different sources which differ quite dramatically. We are unable to offer any reasonable explanation for these discrepancies (highlighted in Section 2).

5.4 Non-Gaussianity of errors

In the MCMC analysis performed in Section 4, we have assumed that the errors on the stellar radius, rotation period and $v \sin i$ measurements are Gaussian in nature. This assumption, however, may not be true, especially given the range of systematic errors that may exist as discussed above. While we could, technically, inject non-Gaussian errors and assume modified probability distributions for each of the parameters in our MCMC analysis, any such probability distribution would have to be guessed at. We feel that, given the complexity and interplay arising due to the systematics discussed above, any such attempt might be just as misleading as our assumption of Gaussianity.

6 TRANSITING SYSTEMS AND TRANSITING PROBABILITIES

The transiting planets included in our literature search are summarized in Table 5 and provide a good test of how accurate our method is, since all these systems should have $\sin i \sim 1$. Indeed, six out of the 11 transiting systems have $\sin i$'s > 0.9, and 10 out of the 11 are within 2σ of $\sin i = 1$. The notable exception is OGLE-TR-111, which yields a wildly discrepant value of $\sin i = 4.518$, probably due to systematic errors in measuring the stellar parameters due to its faintness (see Appendix A for more details). This probably also explains why we obtain a relatively low $\sin i = 0.763$ for OGLE-TR-113. In addition, the extra-solar planet host star HAT-P-1 gives a low $\sin i = 0.747$, but in this case it is actually the member of a binary system and no $B - V$ value is available for the individual

Table 5. Summary of known transiting planets. All the listed sin *i*'s are from the MCMC analysis, except OGLE-TR-111b which was not included in the MCMC analysis on account of its discrepant sin *i* value. The two-tailed 1σ error bars on $\sin i$, σ_- and σ_+ are also listed. The final column indicates the transit probability as calculated from the MCMC analysis, where available.

Name	sin *i*	σ_-	σ_+	Trans. prob.
HAT-P-1b	0.747	0.123	0.141	0.014
HAT-P-2b	0.989	0.069	0.010	0.104
HD17156	0.754	0.165	0.177	0.011
HD189733b	0.933	0.131	0.061	0.075
HD209458b	0.999	0.040	0.000	0.186
OGLE-TR-10b	0.809	0.154	0.178	0.068
OGLE-TR-56b	0.999	0.134	0.000	0.219
OGLE-TR-111b	4.518	1.165	1.165	...
OGLE-TR-113b	0.763	0.191	0.201	0.082
TrES-1b	0.970	0.091	0.029	0.081
TrES-2b	0.986	0.188	0.013	0.081

host star. We calculated a $B-V$ value using $T_{\rm eff} = 5975$ K from Bakos et al. (2007a) and the relationship $\log T_{\rm eff} = 3.908$–0.234 $(B-V)$ from Noyes et al. (1984). It is, therefore, probable that the rotation period we have calculated from $\log R'_{\rm HK}$ and our estimated $(B-V)$ colour is incorrect. Finally, we find a low sin *i* of $0.754^{+0.177}_{-0.165}$ for the transiting system HD 17156. This infers a misalignment angle between the spin-axis of the host star and the orbit of the planet of $41^{\circ}{}^{+13}_{-21}$, which is greater than the values of the projected misalignment angles of $\lambda = 9\overset{\circ}{.}4 \pm 9\overset{\circ}{.}3$ and $10\overset{\circ}{.}0 \pm 5\overset{\circ}{.}1$ reported by Cochran et al. (2008) and Narita et al. (2009*a*), respectively. We note, however, that it is possible to have a truly misaligned system but still measure only a small projected misalignment angle via the Rossiter–McLaughlin effect. Our value for the inclination angle of HD 17156 suggests that this system may yet be misaligned, but this is currently significant at less than the 2σ level.

The remainder of the transiting extra-solar planet host stars, however, all yield sin *i*'s close to 1, with the TrES candidates providing particularly encouraging results. It is comforting to find that eight of the known transiting extra-solar planets in our sample (excluding OGLE-TR-111b, HAT-P-1b and HD 17156 for the reasons outlined earlier) lie within the top 20 transiting candidates as determined from our MCMC analysis. Furthermore, the technique flagged the known transiting extra-solar planet OGLE-TR-56b as the most likely to transit. This suggests that the use of MCMC could be an efficient tool in identifying extra-solar planet transit candidates from spectroscopic analysis of the host stars.

In Table 6, we have listed the top 20 spectroscopically discovered extra-solar planets with the highest transit probabilities as determined from the MCMC analysis. Naturally, there is a bias for extra-solar planets with short orbital periods to be flagged as more probable transit candidates on account of their close proximity to the host star. This means that any long-period extra-solar planet that has a relatively high transit probability is worthy of mention, since such planets are more likely to have been overlooked in targeted transit searches. From Table 6, HD 117176b is perhaps the most interesting candidate. With an orbital period of 116.689 d it would be of no surprise if transits had been missed.

Table 6. The 20 most probable transiting extra-solar planets as determined from spectroscopic data and the MCMC analysis. Only spectroscopically discovered planets are included in this table. Column 1 gives the common name for the extra-solar planet, Column 2 the extra-solar planet's orbital period in days and Column 3 the transit probability as determined from the MCMC analysis.

Name	$P_{\rm orb}$ (d)	Trans. prob.
HD 212301b	2.457	0.182
HD 88133b	3.41	0.166
HD 75289b	3.51	0.148
HD 219828b	3.8335	0.110
τ Boo-b	3.3135	0.109
51 Peg	4.230 77	0.106
HD 187123b	3.097	0.095
HD 38529b	14.309	0.079
CS Pyx-b	2.548 58	0.077
HD 109749b	5.24	0.077
HD 83443b	2.985 625	0.069
HD 179949b	3.0925	0.065
HD 46375b	3.024	0.058
HD 2638b	3.4442	0.055
HD 76700b	3.971	0.049
HD 108147b	10.901	0.032
HD 195019	18.201 63	0.029
HD 330075b	3.369	0.028
HD 117176	116.689	0.017
HD 74156	51.65	0.016

7 RESULTS

For the purposes of this paper, we have adopted the Working Group on Extra-solar Planets definition of a planet to be an object below the limiting mass for thermonuclear fusion of deuterium, currently calculated to be $13M_{\rm J}$. It is comforting, therefore, to find that only six extra-solar planet candidates in our sample have calculated masses that place them over this deuterium burning limit. These are HD 81040b ($17.1M_{\rm J}$), HD 136118b ($14.5M_{\rm J}$), HD 141937b ($17.6M_{\rm J}$), HD 162020b ($147.8M_{\rm J}$), HD 168443c ($18.1M_{\rm J}$) and HD 202206b ($17.7M_{\rm J}$). Of these six, HD 168443c and HD 202206b already had minimum masses calculated to be $> 17.4M_{\rm J}$. Of the remainder, only HD 162020b has a revised mass that puts it significantly above the $13M_{\rm J}$ cut-off for planetary status and, with a calculated true mass of $148M_{\rm J}$, we suggest that the companion is most likely an ∼M4 dwarf. Including the errors on sin *i*, we find a possible minimum mass (at the 1σ level) of $67M_{\rm J}$, and thus the possibility of a brown dwarf companion cannot be ruled out. We believe that a companion mass much larger than $148\ M_{\rm J}$ is unlikely since it would have a clear spectral signature. Interestingly, Udry et al. (2002) use tidal dissipation arguments to conclude that the companion to HD 162020 is probably a brown dwarf, although they could also not rule out a low-mass star, in agreement with our results.

Fig. 1 shows a histogram of the cos *i* values obtained from the MCMC analysis for the spectroscopically discovered systems in our catalogue. This shows a peak at high inclinations where the systems with naive estimators of $\sin i > 1$ pile up at $\sin i = 1$ in the subsequent MCMC analysis. Given an isotropic distribution of stellar rotation inclination angles, one would expect the cos *i* distribution to be flat. However, since the amplitude of a planets' radial velocity signal decreases with sin *i* then we would expect planet detectability to also drop off towards low sin *i*. There does, however, seem to be a slight excess of low inclination systems, with a general decrease in the number of systems populating higher inclinations (ignoring the pile-up). We interpret this overall shape of the distribution to be due to systematic errors pushing high and moderately inclined stars into the $\cos i = 0$ 'spike'. Indeed, one could envisage redistributing

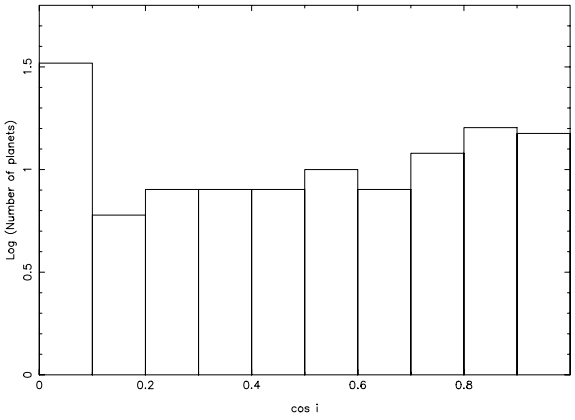

Figure 1. A logarithmic histogram of the cos i values for the spectroscopically discovered extra-solar planet systems in our sample.

the cos $i \sim 0$ systems to lower inclinations, thereby flattening out the observed distribution.

This gives us some confidence that our rejection of stars with naive sin i estimates greater than 1σ above sin $i = 1$ is reasonable. Inclusion of more objects with naive estimates of sin $i > 1$ in the MCMC analysis would simply produce a large number of systems with sin i very close to 1 and very small sin i uncertainties on account of enforcing our prior knowledge that sin < 1. For these reasons, inclusion of these objects would be questionable as it is likely that the errors have been underestimated for these objects, or they are affected by systematics.

A summary of our findings is presented in Fig. 2, which shows both the minimum extra-solar planet masses and 'true' masses versus properties such as number frequency, orbital semimajor axis, orbital eccentricity and host star metallicity. In order to make the comparison fair, we only plot the minimum extra-solar planet masses for those planets which have been included in the MCMC analysis (i.e. only those systems presented in Table 4).

Comparing the results of the minimum and true extra-solar planet masses versus number frequency (top panel, Fig. 2), we still find that lower mass extra-solar planets are more common, with a tail of high-mass companions. This mass distribution can be roughly characterized by the power-law $\mathrm{d}N/\mathrm{d}M \propto M^{-1.1}$ (Butler et al. 2006), and does not change appreciably once the sin i dependency has been removed. This has previously been noted in a purely statistical analysis of extra-solar planet masses by Jorissen, Mayor & Udry (2001). It is often cited (e.g. Jorissen et al. 2001) that the number of planets with minimum masses above $10M_{\rm J}$ is essentially zero – suggesting that planetary formation is a distinct process from that which forms low-mass and sub-stellar (e.g. brown dwarf) objects. When considering their true masses, the planet frequency appears to drop to zero around a slightly higher limit of $\sim 13M_{\rm J}$. Interestingly, this corresponds to the adopted upper mass-limit for a planet at the planet/brown dwarf boundary. Given the low number of extra-solar planets in this mass range, however, it is difficult to definitively place a higher mass 'cut-off' for extra-solar planets.

Figs 2(c) and (d) show the extra-solar planet minimum masses and true masses versus orbital eccentricity, respectively. It can be seen that when considering just the extra-solar planet minimum masses, there is a dearth of low eccentricity ($e < 0.2$) extra-solar planets for minimum masses greater than $\sim 6M_{\rm J}$, as already noted by several other authors (e.g. Butler et al. 2006). When one considers the true masses, however, we find six extra-solar planets with masses in the range 6–$12M_{\rm J}$, along with one brown dwarf companion (all indicated by triangular markers), with $e \sim 0.2$.

These high-mass, low-eccentricity (HMLE) planets are also indicated in Fig. 2(f) which plots semimajor axis versus true extra-solar planet mass. We find that these HMLE extra-solar planets have a wide range of semimajor axes, including one that has one of the largest semimajor axes included in our sample. Therefore, one presumably cannot just appeal to orbital circularization through tidal forces due to the planet's close proximity to the host star to explain these HMLE extra-solar planets.

We have applied the Hartigan dip-test (Hartigan & Hartigan 1985) to check for the non-unimodality of the distribution of orbital eccentricities for exoplanets with masses greater than $5M_{\rm J}$, rejecting objects above $13M_{\rm J}$. This returns a 55 per cent probability that the eccentricity distribution is not unimodal and may, therefore, be indicative of two different populations of exoplanets. A larger sample of extra-solar planets in the $>5M_{\rm J}$ mass range is needed before any firm conclusions about the significance of these HMLE extra-solar planets can be drawn. A larger sample of high-mass extra-solar planets would also help to establish whether the gap in orbital eccentricities between $e = 0.2$ and 0. 3 for high-mass extra-solar planets apparent in Fig. 2(d) is real. If confirmed, however, the presence of these HMLE extra-solar planets, and the gap in orbital eccentricities between $e = 0.2$ and 0. 3, hints at a distinct evolution and/or formation process for these extra-solar planets.

Studies of brown dwarfs and spectroscopic binaries have shown that they exhibit a similar eccentricity distribution to the higher mass extra-solar planets (extra-solar planets exhibit a trend of increasing mean orbital eccentricity with increasing mass, as mentioned earlier). This has led Ribas & Miralda-Escudé (2007) to suggest that the eccentricity-mass distribution of extra-solar planets may provide a signature of different extra-solar planet formation mechanisms. They hypothesize that there are two formation scenarios for extra-solar planets. The first is that the low-mass population forms by gas accretion on to an ice-rock core within the circumstellar disc, and initially form in circular orbits and grow their eccentricities by varying amounts later. The second is that the high-mass population forms directly from fragmentation of the pre-stellar cloud (in the same manner as brown dwarfs and binaries) and would initially be located in far larger orbits. The subsequent long-distance migration required to bring them to their current positions is then postulated to drive these higher mass extra-solar planets to much larger eccentricities.

If Ribas & Miralda-Escudé (2007) are correct then this might suggest that the candidates we have identified as HMLE extra-solar planets in Fig. 2 have formed along the same route as the low-mass planets, i.e. through gas accretion on to a rock-ice core rather than via fragmentation. In order to form such massive planets by gas accretion, we might expect the host stars to have higher metallicities. Figs 2(g) and (h) show host star metallicity [Fe/H] versus M sin i and true mass, respectively, with the HMLE extra-solar planets indicated by triangles. We note that five of the HMLEs are indeed around host stars with high metallicities but the remaining HMLE candidate happens to be around one of the most-metal poor host stars in our selection. The anonymous referee has pointed out that the conclusion that the HMLEs should have higher metallicities is not the only possibility, and that the formation in a high-mass disc could supply the right environmental conditions as well. Obviously, the true masses of more extra-solar planets need to be calculated before any sound conclusions as to whether these HMLEs truly constitute a distinct population, and the clues they may give us about planetary formation, can be made.

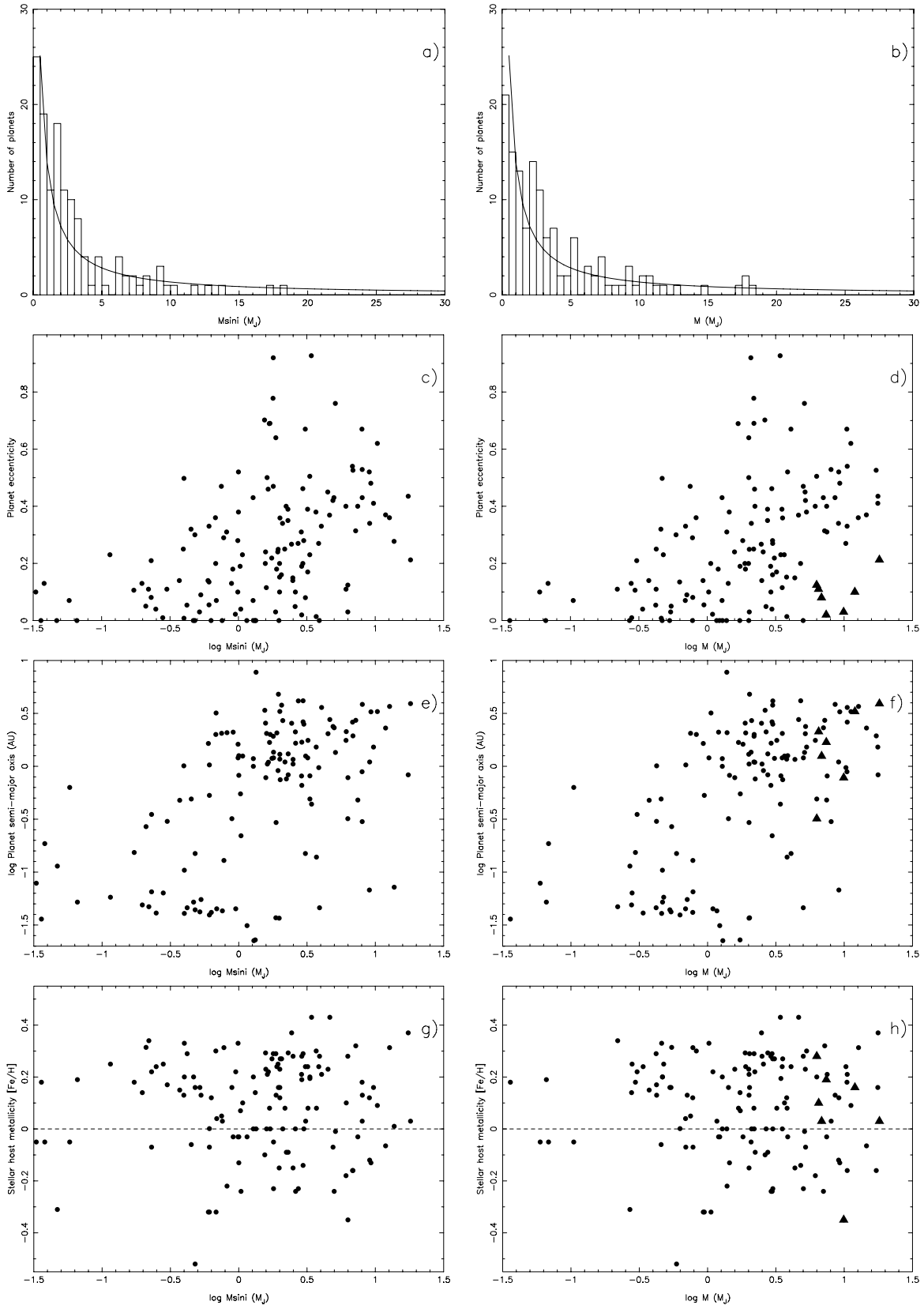

Figure 2. Top panel: a histogram of the number of extra-solar planets with (a) observed minimum masses $M \sin i$ and (b) their calculated true masses, M (both in units of Jupiter masses, M_J). The solid line indicates a mass distribution characterized by the power-law $\mathrm{d}N/\mathrm{d}M \propto M^{-1.1}$. (c) and (d): the orbital eccentricity versus the minimum extra-solar planet mass and their calculated true masses, respectively. A number of relatively high-mass, low eccentricity ($e < 0.25$) planets discussed in Section 7 have been indicated using triangular markers. Figs 2(e) and (f) are the same as (c) and (d), but against extra-solar planet semimajor axis. Finally, figures (g) and (h) plot the host star metallicity [Fe/H] versus $M \sin i$ and true mass. The horizontal dashed line represents solar metallicity.

8 DISCUSSION AND CONCLUSIONS

Under the assumption that the rotation axes of extra-solar planet host stars are aligned perpendicularly to the planes of the extra-solar planetary orbits, we have used measurements of R_*, $v \sin i$ and $P_{\rm rot}$ to remove the $\sin i$ dependency from 133 spectroscopically determined extra-solar planet mass determinations. We find that, bar two problematic cases, the inclination angles of all the known transiting extra-solar planets in our sample are commensurate with $\sin i = 1$, as expected. Using an MCMC analysis, we have also computed the transit probabilities of all 133 extra-solar planets from purely spectroscopic measurements. We find that all eight known transiting extra-solar planets with reliable parameter determinations lie in the top 20 most probable transiting candidates. This gives us some confidence that not only can the technique outlined in this paper be used to correctly estimate the true masses of extra-solar planets, but also that MCMC can reliably identify extra-solar planet transit candidates from spectroscopic measurements.

We find that only six out of the 133 extra-solar planets have masses that place them over the standard $13 M_{\rm J}$ upper limit for planets, which indicates that the vast majority of extra-solar planet candidates found by spectroscopic means are truly planetary in nature. We also find evidence for a population of high-mass extra-solar planets with low orbital eccentricities that is not apparent when only extra-solar planet minimum masses are considered. It is possible that these extra-solar planets may have formed along a different path to the other high-mass extra-solar planets. This suggests that, while some high-mass planets may well form through fragmentation resulting in high eccentricity orbits as suggested by Ribas & Miralda-Escudé (2007), not all high-mass planets form in this way.

Only by calculating the true masses of more extra-solar planets can such distributions, and their impact on our understanding of both planet *and* brown dwarf formation, be properly studied. With 453 extra-solar planet candidates, there are still over 300 extra-solar planets for which we could not find the necessary data to determine $\sin i$, or for which the data were unreliable and yielded $\sin i$'s significantly greater than 1. There are several observational problems to overcome. In order to calculate the rotation period of the star we generally must rely on measurements of the strength of the chromospheric Ca II H & K lines and apply the chromospheric-emission/rotation law of Noyes et al. (1984). The Noyes et al. (1984) relation has obvious drawbacks (i.e. it is not a direct measurement of the stellar rotation period), and the Ca II H & K emission in these stars may be variable over long-time-scales due to, for example, magnetic activity cycles like the 11-year solar cycle. Thus measurements of Ca II H & K need to be averaged over a suitably long time-span in order to derive a reliable rotation period. Whilst we are in the fortunate position that large Ca II H & K surveys like the Mt. Wilson survey have observed many extra-solar planet host stars for several decades now, there are still many host stars where only one brief 'snapshot' of the chromospheric emission is available from the planet discovery paper. We plan to commence the targeted monitoring of chromospheric emission from extra-solar planet host stars, not only to obtain a long-term average of the chromospheric emission from these stars, but also to see if variations in the indicators over the *actual* rotation period of the star can be identified. This would give a direct measure of the stellar rotation period.

The next observational problem is the determination of the projected stellar equatorial velocity, $v \sin i$. Again, the nature of the hunt for extra-solar planets means that the host stars are almost always observed with high-resolution echelle spectrographs from which the line-broadening can be measured. Due to the low (typically $\sim 2\,{\rm km\,s^{-1}}$) rotation velocities of these stars, rotational broadening is no longer the dominant line-broadening mechanism, and other mechanisms such as thermal broadening and turbulence need to be taken into account. Many of the quoted $v \sin i$ measurements in the literature do not fully account for these effects, which require the use of stellar atmosphere models to estimate the true level of broadening due to rotation. We plan to systematically analyse the spectra of extra-solar planet host stars to produce accurate $v \sin i$ measurements taking into account other broadening mechanisms.

Finally, we note that the inclination of the rotation axis of stars can be measured using asteroseismology. Gizon & Solanki (2003) present a technique which determines the stellar axial inclination from observations of low-degree non-radial oscillations which are strong functions of i. They find that the inclination angle can be measured using this method to within $\sim 10^\circ$ when $i > 30^\circ$. One condition for this technique to work, however, is that the star must have a high-rotation rate, and this restricts the technique to stars that rotate at least twice as fast as the Sun. Since the host stars of extra-solar planets are generally slow rotators (selected in order to avoid 'jitter' in the radial velocity measurements caused by magnetic activity which is enhanced for more rapidly rotating stars), this technique will not be able to access a substantial portion of these stars. We therefore believe that, for the foreseeable future at least, the technique outlined in this paper will remain the main way in which to remove the $\sin i$ degeneracy in spectroscopically determined extra-solar planet masses.

ACKNOWLEDGMENTS

Much of this work was carried out while CAW was supported by a PPARC/STFC Postdoctoral Fellowship. SPL acknowledges the support of an RCUK fellowship. The authors would also like to thank the anonymous referee whose detailed and valuable comments substantially helped us improve the quality of this paper.

REFERENCES

Acke B., Waelkens C., 2004, A&A, 427, 1009
Alonso R. et al., 2004, ApJ, 613, L153
Anderson D. R. et al., 2010, ApJ, 709, 159
Bakos G. Á. et al., 2007a, ApJ, 656, 552
Bakos G. Á. et al., 2007b, ApJ, 670, 826
Barnes S. A., 2001, ApJ, 561, 1095
Barnes S. A., 2007, ApJ, 669, 1167
Barnes J. R., Collier Cameron A., James D., Donati J.-F., 2001, MNRAS, 324, 231
Beck J. G., Giles P., 2005, ApJ, 621, L153
Benz W., Mayor M., 1984, A&A, 138, 183
Bernacca P. L., Perinotto M., 1970, Contributions dell'Osservatorio Astrofisica dell'Universita di Padova in Asiago, 239, 1
Bernkopf J., Fidler A., Fuhrmann K., 2001, in von Hippel T., Simpson C., Manset N., eds, ASP Conf. Ser. Vol. 245, Astrophysical Ages and Times Scales. The Dark Side of the Milky Way. Astron. Soc. Pac., San Francisco, p. 207
Beuermann K., Baraffe I., Hauschildt P., 1999, A&A, 348, 524
Bouchy F., Pont F., Santos N. C., Melo C., Mayor M., Queloz D., Udry S., 2004, A&A, 421, L13
Bouchy F. et al., 2005, A&A, 444, L15
Bouchy F. et al., 2008, A&A, 482, L25
Brown T. M., 2010, ApJ, 709, 535
Butler R. P., Vogt S. S., Marcy G. W., Fischer D. A., Henry G. W., Apps K., 2000, ApJ, 545, 504

Butler R. P., Marcy G. W., Vogt S. S., Fischer D. A., Henry G. W., Laughlin G., Wright J. T., 2003, ApJ, 582, 455
Butler R. P. et al., 2006, ApJ, 646, 505
Cameron A. C., Donati J.-F., 2002, MNRAS, 329, 23
Cameron A. C., Foing B. H., 1997, Observatory, 117, 218
Cochran W. D., Redfield S., Endl M., Cochran A. L., 2008, ApJ, 683, L59
Collier Cameron A. et al., 2007, MNRAS, 380, 1230
Da Silva R. et al., 2006, A&A, 446, 717
de Medeiros J. R., Mayor M., 1999, A&AS, 139, 433
di Benedetto G. P., Rabbia Y., 1987, A&A, 188, 114
Eggenberger A., Mayor M., Naef D., Pepe F., Queloz D., Santos N. C., Udry S., Lovis C., 2006, A&A, 447, 1159
Fischer D. A., Valenti J., 2005, ApJ, 622, 1102
Fischer D. A., Marcy G. W., Butler R. P., Vogt S. S., Frink S., Apps K., 2001, ApJ, 551, 1107
Fischer D. A., Marcy G. W., Butler R. P., Vogt S. S., Walp B., Apps K., 2002, PASP, 114, 529
Fischer D. A. et al., 2006, ApJ, 637, 1094
Fischer D. A. et al., 2007, ApJ, 669, 1336
Ford E. B., 2006, ApJ, 642, 505
Fouque P., Gieren W. P., 1997, A&A, 320, 799
Fracassini L. E. P., Pastori L., Covino S., Pozzi A., 2001, A&A, 367, 521
Fuhrmann K., 1998, A&A, 338, 161
Fuhrmann K., Pfeiffer M. J., Bernkopf J., 1997, A&A, 326, 1081
Fuhrmann K., Pfeiffer M. J., Bernkopf J., 1998, A&A, 336, 942
Galland F., Lagrange A.-M., Udry S., Chelli A., Pepe F., Beuzit J.-L., Mayor M., 2005, A&A, 444, L21
Gaudi B. S., Winn J. N., 2007, ApJ, 655, 550
Ge J. et al., 2006, ApJ, 648, 683
Gillon M. et al., 2009, A&A, 501, 785
Gizon L., Solanki S. K., 2003, ApJ, 589, 1009
Gonzalez G., 1998, A&A, 334, 221
Gregory P. C., 2007, MNRAS, 374, 1321
Hartigan J. A., Hartigan P. M., 1985, Ann. Statistics, 13, 70
Hatzes A. P. et al., 2006, A&A, 457, 335
Hébrard G. et al., 2008, A&A, 488, 763
Henry T. J., Soderblom D. R., Donahue R. A., Baliunas S. L., 1996, AJ, 111, 439
Henry G. W., Baliunas S. L., Donahue R. A., Fekel F. C., Soon W., 2002a, AJ, 531, 415
Henry G. W., Donahue R. A., Baliunas S. L., 2002b, ApJ, 577, L111
Irwin J. et al., 2008, ApJ, 681, 636
Jenkins J. S. et al., 2006, MNRAS, 3372, 163
Jenkins J. M. et al., 2010, preprint (arXiv:1001.0416)
Johnson J. A. et al., 2006a, ApJ, 647, 600
Johnson J. A., Marcy G. W., Fischer D. A., Henry G. W., Wright J. T., Isaacson H., McCarthy C., 2006b, ApJ, 652, 1724
Johnson J. A. et al., 2007, ApJ, 665, 785
Johnson J. A. et al., 2008, ApJ, 686, 649
Johnson J. A., Winn J. N., Albrecht S., Howard A. W., Marcy G. W., Gazak J. Z., 2009, PASP, 121, 1104
Jones H. R. A., Butler P. R., Tinney C. G., Marcy G. W., Penny A. J., McCarthy C., Carter B. D., 2003, MNRAS, 341, 948
Jones H. R. A., Butler R. P., Tinney C. G., Marcy G. W., Carter B. D., Penny A. J., McCarthy C., Bailey J., 2006, MNRAS, 369, 249
Jorissen A., Mayor M., Udry S., 2001, A&A, 379, 992
Konacki M. et al., 2004, ApJ, 609, L37
Konacki M., Torres G., Sasselov D. D., Jha S., 2005, ApJ, 624, 372
Korzennik S. G., Brown T. M., Fischer D. A., Nisenson P., Noyes R. W., 2000, ApJ, 533, L147
Laughlin G., Wolf A., Vanmunster T., Bodenheimer P., Fischer D., Marcy G., Butler P., Vogt S., 2005, ApJ, 621, 1072
Lo Curto G. et al., 2006, A&A, 451, 345
Lovis C. et al., 2005, A&A, 437, 1121
Lovis C. et al., 2006, Nat, 441, 305
Lowrance P. J. et al., 2005, AJ, 130, 1845
Malmberg D., Davies M. B., Chambers J. E., 2007, MNRAS, 377, L1
Marcy G. W., Butler R. P., Fischer D. A., Laughlin G., Vogt S. S., Henry G. W., Pourbaix D., 2002, ApJ, 581, 1375
Masana E., Jordi C., Ribas I., 2006, A&A, 450, 735
Mayor M., Queloz D., 1995, Nat, 378, 355
Mayor M., Udry S., Naef D., Pepe F., Queloz D., Santos N. C., Burnet M., 2004, A&A, 415, 391
Mazeh T. et al., 2000, ApJ, 532, L55
Melo C., Santos N. C., Pont F., Guillot T., Israelian G., Mayor M., Queloz D., Udry S., 2006, A&A, 460, 251
Melo C. et al., 2007, A&A, 467, 721
Messina S., Rodonò M., Guinan E. F., 2001, A&A, 366, 215
Moutou C. et al., 2005, A&A, 439, 367
Naef D. et al., 2001, A&A, 375, L27
Naef D. et al., 2003, A&A, 410, 1051
Naef D., Mayor M., Beuzit J. L., Perrier C., Queloz D., Sivan J. P., Udry S., 2004, A&A, 414, 351
Naef D. et al., 2007, A&A, 470, 721
Narita N. et al., 2007, PASJ, 59, 763
Narita N., Sato B., Oshima O., Winn J. N., 2008, PASJ, 60, 1
Narita N. et al., 2009a, PASJ, 61, 991
Narita N., Sato B., Hirano T., Tamura M., 2009b, PASJ, 61, L35
Narita N., Sato B., Hirano T., Winn J. N., Aoki W., Tamura M., 2010, PASJ, 62, 653
Nordström B. et al., 2004, A&A, 418, 989
Noyes R. W., Hartmann L. W., Baliunas S. L., Duncan D. K., Vaughan A. H., 1984, ApJ, 279, 763
O'Toole S. J. et al., 2007, ApJ, 660, 1636
Pepe F., Mayor M., Galland F., Naef D., Queloz D., Santos N. C., Udry S., Burnet M., 2002, A&A, 388, 632
Pepe F. et al., 2004, A&A, 423, 385
Perrier C., Sivian J. P., Naef D., Beuzit J. L., Mayor M., Queloz D., Udry S., 2003, A&A, 410, 1039
Pizzolato N., Maggio A., Micela G., Sciortino S., Ventura P., 2003, A&A, 397, 147
Pont F. et al., 2007, A&A, 465, 1069
Pont F. et al., 2009, A&A, 502, 695
Queloz D., Eggenberger A., Mayor M., Perrier C., Beuzit J. L., Naef D., Sivan J. P., Udry S., 2000, A&A, 359, L13
Queloz D. et al., 2010, A&A, 517, L1
Reiners A., Schmitt J. H. M. M., 2003, A&A, 398, 647
Ribas I., Miralda-Escudé J., 2007, A&A, 464, 779
Saar S. H., Osten R. A., 1997, MNRAS, 284, 803
Saffe C., Gómez M., Chavero C., 2005, A&A, 443, 609
Santos N. C., Mayor M., Naef D., Pepe F., Queloz D., Udry S., Blecha A., 2000, A&A, 361, 265
Santos N. C., Mayor M., Naef D.and Pepe F., Queloz D., Udry S., Burnet M., 2001, A&A, 379, 999
Santos N. C. et al., 2002, A&A, 392, 215
Santos N. C. et al., 2004, A&A, 426, L19
Santos N. C. et al., 2006, A&A, 450, 825
Sato B. et al., 2003, ApJ, 597, L157
Simpson E. K. et al., 2010, MNRAS, 405, 1867
Skelly M. B., Unruh Y. C., Barnes J. R., Lawson W. A., Donati J.-F., Collier Cameron A., 2009, MNRAS, 399, 1829
Soderblom D. R., 1982, ApJ, 263, 239
Sozzetti A. et al., 2004, ApJ, 616, L167
Sozzetti A. et al., 2006, A&A, 449, 417
Sozzetti A., Torres G., Charbonneau D., Latham D. W., Holman M. J., Winn J. N., Laird J. B., O'Donovan F. T., 2007, ApJ, 664, 1190
Strassmeier K. G., Washuetti A., Granzer T., Scheck M., Weber M., 2000, A&AS, 142, 275
Takeda G., Rasio F. A., 2005, ApJ, 627, 1001
Tegmark M. et al., 2004, Phys. Rev. D., 69, 103501
Tingley B., Sackett P. D., 2005, AJ, 627, 1011
Torres G., Winn J. N., Holman M. J., 2008, ApJ, 677, 1324
Triaud A. H. M. J. et al., 2009, A&A, 506, 377
Triaud A. H. M. J. et al., 2010, preprint (arXiv:1008.2353)

Udry S., Mayor M., Naef D., Pepe F., Queloz D., Santos N. C., Burnet M., 2002, A&A, 390, 267
Udry S. et al., 2003, A&A, 407, 679
Udry S. et al., 2006, A&A, 447, 361
Valenti J. A., Fischer D. A., 2005, ApJS, 159, 141
Vaughan A. H., Baliunas S. L., Middelkoop F., Hartmann L. W., Mihalas D., Noyes R. W., Preston G. W., 1981, ApJ, 250, 276
Vogt S. S., Butler R. P., Marcy G. W., Fischer D. A., Pourbaix D., Apps K., Laughlin G., 2002, ApJ, 568, 352
Watson C. A., Dhillon V. S., Shabaz T., 2006, MNRAS, 368, 637
Watson C. A., Steeghs D., Shabaz T., Dhillon V. S., 2007, MNRAS, 382, 1105
Wilson O. C., 1978, ApJ, 226, 379
Winn J. N. et al., 2005, ApJ, 631, 1215
Winn J. N. et al., 2007, ApJ, 665, L167
Winn J. N. et al., 2008, ApJ, 682, 1283
Winn J. N. et al., 2009a, ApJ, 700, 302
Winn J. N. et al., 2009b, ApJ, 703, 2091
Wolf A. S., Laughlin G., Henry G. W., Fischer D. A., Marcy G., Butler P., Vogt S., 2007, ApJ, 667, 549
Wolszcan A., Frail D. A., 1992, Nat, 355, 145
Wright J. T., Marcy G. W., Butler P. R., Vogt S. S., 2004, ApJS, 152, 261

APPENDIX A: NOTES ON SPECIFIC SYSTEMS WITH SIN *i* GREATER THAN 1

From Tables 3 and 4 we can see that out of a total of 154 extra-solar planet hosts with sufficient data, 119 (77 per cent) yield $\sin i < 1$ or are within 1σ of $\sin i = 1$. In this section we discuss why some systems have calculated $\sin i$'s significantly (i.e. more than 1σ) greater than 1.

Sub-giants

Of the 35 extra-solar planet host stars with $\sin i$ significantly greater than 1, ten are classified as sub-giants. Since the Noyes et al. (1984) chromospheric index–rotation rate relationship is calibrated for main-sequence stars only, we believe that the rotation periods of these stars determined from $R'_{\rm HK}$ measurements may be incorrect. We have indicated the sub-giants with asterisks in Table 3. Other systems where we can highlight potential problems which may result in values of $\sin i > 1$ are discussed briefly below.

A1 HD 142

In addition to being classified as a sub-giant, the $(B - V)$ colour of this star may be contaminated by a nearby companion as reported by the NStED data base.

HD 11506

We note that Fischer et al. (2007) quote the stellar rotation period determined from the $\log R'_{\rm HK}$ measurements is 12.6 d. We, however, derive a longer rotation period of 18.3 d using the $\log R'_{\rm HK}$ value reported by Fischer et al. (2007) and the relationship from Noyes et al. (1984). We therefore believe the rotation period quoted by Fischer et al. (2007) has been calculated incorrectly.

HD 13445

There seems to be some confusion over the $v \sin i$ value for this star. Fischer & Valenti (2005) quote $2.37\,{\rm km\,s^{-1}}$, while Saar & Osten (1997) place an upper limit of $0.7\,{\rm km\,s^{-1}}$. Assuming a $v \sin i$ of $2.37\,{\rm km\,s^{-1}}$ results in a large $\sin i \sim 1.8$, while adopting the limit of $0.7\,{\rm km\,s^{-1}}$ gives $\sin i \sim 0.5$. Given the doubt over $v \sin i$ for this star we have deemed this measurement to be suspect.

HD 27442

There is considerable doubt over the radius of this star, with estimates ranging from 3.48 to $6.60\,{\rm R_\odot}$. Furthermore, this star is classified as a sub-giant, hence the rotation period derived from the $\log R'_{\rm HK}$ measurements is also likely to be inaccurate.

HD 27894

This has an uncertain $v \sin i$, with only an upper limit of $1.5\,{\rm km\,s^{-1}}$ from Moutou et al. (2005).

HD 28185

This has an uncertain $v \sin i$, with estimates ranging from 1.82 to $3.00\,{\rm km\,s^{-1}}$. While $v \sin i = 1.82\,{\rm km\,s^{-1}}$ gives $\sin i = 1$, we feel there is too much uncertainty in the $v \sin i$ values, and hence have taken a weighted mean, placing HD 28185 in the $\sin i$ significantly greater than 1 category.

HD 75732

The calculated rotational period of the star from $\log R'_{\rm HK}$ measurements (42–47 d) is possibly related to the orbit of one of its planets, 55 Cnc c, which has a measured orbital period of 43.93 d (see Marcy et al. 2002).

HD 86081

We note that Johnson et al. (2006a) derived a stellar rotation period of 40.1 d from their measured $\log R'_{\rm HK}$ using the calibration of Noyes et al. (1984). Employing the same $B - V$ colour and $\log R'_{\rm HK}$ quoted by Johnson et al. (2006a) we determine a far shorter rotation period of 27.7 d via the same relationship, and 24.83 d if we take the value of $B - V = 0.641$ from the NStED data base. We therefore conclude that the rotation period derived by Johnson et al. (2006a) is incorrect but, despite the shorter rotation period we have calculated, we still determine $\sin i = 1.590$.

HD 145675

While Fischer & Valenti (2005) quote a $v \sin i = 1.56\,{\rm km\,s^{-1}}$, Naef et al. (2004) quote an upper limit of $v \sin i < 1\,{\rm km\,s^{-1}}$. This upper limit would yield $\sin i < 0.832$. Given the apparent doubt over $v \sin i$ we have decided to place this object in the $\sin i$ significantly greater than 1 category.

HD 246435

Jones et al. (2003) have noted a discrepancy between the assigned spectral-type of HD 216435 in the literature, which is either quoted as G0V or G3IV. They find that HD 216435 lies 1 mag above the main sequence, and hence this star is most likely a sub-giant. The rotation period determined from $\log R'_{\rm HK}$ is therefore suspect.

OGLE-TR-111

While the OGLE extra-solar planets are all transiting systems, published data for OGLE-TR-111 yield a $\sin i = 4.518 \pm 0.486$ and is one of the most discrepant systems found in this work. We believe that this is undoubtedly due to the faintness of the OGLE targets (all OGLE extra-solar planet hosts have $I > 14$ whereas most extra-solar planet hosts typically have V-band magnitudes around 8–9), which means that accurate spectroscopic follow-up is difficult. In addition, none of these systems has a long baseline of $R'_{\rm HK}$ measurements, which means that the rotation periods are also not well known. For these reasons, we believe that systematic errors in one or more of the measurements have contributed to the highly discrepant $\sin i$ obtained for OGLR-TR-111.

Summary

In total, we can find plausible reasons explaining why 18 of the extra-solar planet host stars yield $\sin i$'s significantly greater than 1. This still leaves 17 systems for which no explanation can be given for their high $\sin i$ values.

APPENDIX B: NOTES ON SPECIFIC SYSTEMS WITH SIN *I* LESS THAN 1

In this section, we highlight any published data on stars that appear incorrect, and justify any decisions that have been made regarding the rejection of any published parameters from our analysis. Any other special cases that apply are also indicated here, such as the use of actual observed stellar rotation rates from photometry instead of rotation rates derived from $\log R'_{\rm HK}$ measurements, for example.

HD 1237

The value of $P_{\rm rot} = 12.6$ d quoted on the Geneva Observatory web-page and apparently derived from the Noyes et al. (1984) relationship appears to be wrong. Using the Geneva Observatory's values of $\log R'_{\rm HK} = -4.27$ and $B - V = 0.749$, we derive $P_{\rm rot} = 4.01$ d. We note that Barnes (2001) use the same $B - V$ value, but a weaker chromospheric activity index of $\log R'$ HK $= -4.44$ and derive a rotation period of 10.4 d. Using the values of Barnes (2001), we also derive 10.4 d, and thus conclude that the Geneva $P_{\rm rot}$ is quoted incorrectly.

HD 6464

The Extra-solar Planets Encyclopedia quote the radius of HD 6434 as 0.57 $R_\odot$ (from Fracassini et al. 2001) and its spectral type as G3 IV. The NStED data base quotes the spectral type as G2–3 V. Given the spectral type, we find it highly unlikely that the radius is actually 0.57 $R_\odot$, and instead use the value of 1.0 $R_\odot$ from the NStED data base.

HD 16141

The Extra-solar Planets Encyclopedia quotes a radius for HD 16141 of 1 $R_\odot$ but provides no reference for this figure. Given this, and that the radius is discrepant from other estimates obtained from the literature (1.4 and 1.52 $R_\odot$), we have rejected this radius estimate from Table 1.

HD 142022A

Eggenberger et al. (2006) determined an upper limit of 48 d to the rotation period of HD 142022A by combining their measured $v \sin i$ with the radius of the star estimated from evolutionary models. Despite measuring $\log R'_{\rm HK}$, they did not calculate the rotation period using the Noyes et al. (1984) relationship. Using Eggenberger et al. (2006)'s values for $\log R'_{\rm HK} = -4.97$ and $B - V = 0.790$ we determine a rotation period of 39 d.

HD 170469

Fischer et al. (2007) quote a $\log R'_{\rm HK} = -5.06$ and determine the rotation period to be 13 d. Using the same value of $\log R'_{\rm HK}$, we determine the rotation period to be 30 d. Our period agrees closely with that of Wright et al. (2004), who find a rotation period of 31 d from a very similar measurement of $\log R'_{\rm HK} = -5.09$. We therefore assume that Fischer et al. (2007) have calculated the rotation period incorrectly.

HD 217014

The rotation period of 21.9 d has been used since this is a measured rotation period from variability in the light curve, rather than one estimated from $\log R'_{\rm HK}$.

SUPPORTING INFORMATION

Additional Supporting Information may be found in the online version of this article:

Table 1. Published data on the properties of 154 extra-solar planet host stars.
Table 2. Compilation of chromospheric indices ($\log R'_{\rm HK}$) for the stars in Table 1.

Please note: Wiley-Blackwell are not responsible for the content or functionality of any supporting materials supplied by the authors. Any queries (other than missing material) should be directed to the corresponding author for the article.

This paper has been typeset from a TEX/LATEX file prepared by the author.